Since January 2020 Elsevier has created a COVID-19 resource centre with free information in English and Mandarin on the novel coronavirus COVID-19. The COVID-19 resource centre is hosted on Elsevier Connect, the company's public news and information website.

Cancer Cell

Article

Impaired humoral immunity is associated with prolonged COVID-19 despite robust CD8 T cell responses

Graphical abstract

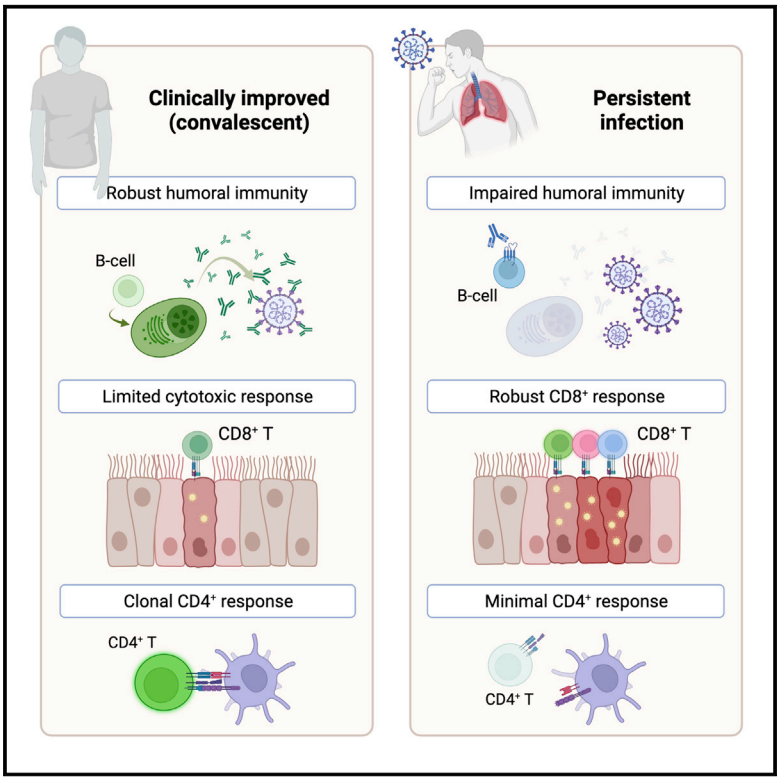

Highlights

- Cancer patients with persistent COVID-19 infection have low humoral immune responses
- Robust CD8$^+$ T cell responses are unable to clear virus in B cell-depleted patients
- Potent CD4$^+$ T cell responses are in B cell-depleted patients with viral clearance

Authors

Olga Lyudovyk, Justin Y. Kim, David Qualls, ..., Benjamin Greenbaum, Alexander C. Huang, Santosha A. Vardhana

Correspondence

greenbab@mskcc.org (B.G.), alexander.huang@pennmedicine.upenn.edu (A.C.H.), vardhans@mskcc.org (S.A.V.)

In brief

Lyudovyk et al. analyze immunological factors required for SARS-CoV-2 clearance in patients with cancer. They observe delayed viral clearance in patients with impaired humoral immunity despite broad and functional antiviral CD8$^+$ T cell responses. However, B cell-deficient patients with robust CD4$^+$ T cell responses were frequently able to achieve efficient viral clearance.

Lyudovyk et al., 2022, Cancer Cell *40*, 738–753
July 11, 2022
https://doi.org/10.1016/j.ccell.2022.05.013

CellPress

CellPress

Cancer Cell

Article

Impaired humoral immunity is associated with prolonged COVID-19 despite robust CD8 T cell responses

Olga Lyudovyk,[1,17] Justin Y. Kim,[2,3,16,17] David Qualls,[4,17] Madeline A. Hwee,[5] Ya-Hui Lin,[5] Sawsan R. Boutemine,[6] Yuval Elhanati,[1] Alexander Solovyov,[1] Melanie Douglas,[4] Eunise Chen,[7] N. Esther Babady,[8,9] Lakshmi Ramanathan,[10] Pallavi Vedantam,[11] Chaitanya Bandlamudi,[11] Sigrid Gouma,[12] Philip Wong,[11] Scott E. Hensley,[3,12] Benjamin Greenbaum,[1,13,*] Alexander C. Huang,[2,3,14,15,*] and Santosha A. Vardhana[4,5,15,18,*]

[1]Computational Oncology, Department of Epidemiology and Biostatistics, Memorial Sloan Kettering Cancer Center, New York, NY, USA
[2]Division of Hematology/Oncology, Department of Medicine, Perelman School of Medicine, University of Pennsylvania, Philadelphia, PA 19104, USA
[3]Institute for Immunology, Perelman School of Medicine, University of Pennsylvania, Philadelphia, PA 19104, USA
[4]Lymphoma Service, Division of Hematologic Malignancies, Department of Medicine, Memorial Sloan Kettering Cancer Center, New York, NY, USA
[5]Human Oncology and Pathogenesis Program, Memorial Sloan Kettering Cancer Center, New York, NY, USA
[6]Department of Medicine, Memorial Sloan Kettering Cancer Center, New York, NY, USA
[7]University of Texas Health Science Center at Houston, McGovern Medical School, Houston, TX, USA
[8]Infectious Diseases Service, Department of Medicine, Memorial Sloan Kettering Cancer Center, New York, NY, USA
[9]Clinical Microbiology Service, Department of Laboratory Medicine, Memorial Sloan Kettering Cancer Center, New York, NY, USA
[10]Clinical Chemistry Service, Department of Laboratory Medicine, Memorial Sloan Kettering Cancer Center, New York, NY, USA
[11]Memorial Sloan Kettering Cancer Center, New York, NY, USA
[12]Department of Microbiology, Perelman School of Medicine, University of Pennsylvania, Philadelphia, PA 19104, USA
[13]Physiology, Biophysics & Systems Biology, Weill Cornell Medicine, Weill Cornell Medical College, New York, NY, USA
[14]Abramson Cancer Center, University of Pennsylvania, Philadelphia, PA 19104, USA
[15]Parker Institute for Cancer Immunotherapy, San Francisco, CA, USA
[16]Present address: Lewis Katz School of Medicine, Temple University, Philadelphia, PA, USA
[17]These authors contributed equally
[18]Lead contact
*Correspondence: greenbab@mskcc.org (B.G.), alexander.huang@pennmedicine.upenn.edu (A.C.H.), vardhans@mskcc.org (S.A.V.)
https://doi.org/10.1016/j.ccell.2022.05.013

SUMMARY

How immune dysregulation affects recovery from COVID-19 infection in patients with cancer remains unclear. We analyzed cellular and humoral immune responses in 103 patients with prior COVID-19 infection, more than 20% of whom had delayed viral clearance. Delayed clearance was associated with loss of antibodies to nucleocapsid and spike proteins with a compensatory increase in functional T cell responses. High-dimensional analysis of peripheral blood samples demonstrated increased $CD8^+$ effector T cell differentiation and a broad but poorly converged COVID-specific T cell receptor (TCR) repertoire in patients with prolonged disease. Conversely, patients with a $CD4^+$ dominant immunophenotype had a lower incidence of prolonged disease and exhibited a deep and highly select COVID-associated TCR repertoire, consistent with effective viral clearance and development of T cell memory. These results highlight the importance of B cells and $CD4^+$ T cells in promoting durable SARS-CoV-2 clearance and the significance of coordinated cellular and humoral immunity for long-term disease control.

INTRODUCTION

Severe acute respiratory syndrome coronavirus 2 (SARS-CoV-2) infection is associated with greater mortality and morbidity in patients with cancer (Dai et al., 2020). While studies have focused predominantly on outcomes in the acute phase, there is increasing evidence that prolonged SARS-CoV-2 infection can have a significant impact on patient outcomes, particularly in patients with compromised immune function at baseline (Lee et al., 2022). Patients receiving B cell-depleting therapy for lymphoid malignancies are at particularly high risk for prolonged disease with delayed clearance of SARS-CoV-2 and subsequent episodes of clinical decompensation (Arcani et al., 2021; Lee et al., 2022). Additionally, delayed viral clearance may contribute to delayed initiation or disruption of cancer-directed therapy, which has been reported during the pandemic and contributes

significantly to mortality in patients with cancer (Clark et al., 2021; Ranganathan et al., 2021; Satish et al., 2021).

Studies describing the role of host immunity in recovery from COVID-19 have predominantly focused on patients with normal immune function and mild cases of infection. These studies have demonstrated broad humoral and cellular adaptive memory in recovered patients (Dan et al., 2021; Kared et al., 2021; Minervina et al., 2021; Peng et al., 2020; Rodda et al., 2021; Sekine et al., 2020). However, the long-term immune response to COVID-19 in patients with immune deficits or delayed viral clearance has not been explored.

We recently demonstrated that during acute COVID-19 infection, $CD8^+$ T cells are a key contributor to acute disease control and are particularly critical in patients lacking B cell function (Bange et al., 2021). We next aimed to understand whether distinct components of the adaptive immune response are critical for long-term viral clearance. Therefore, we asked whether immune deficits from cancer and/or cancer-related therapies altered immune-mediated recovery from COVID-19. We found that a significant proportion of patients with cancer exhibited delayed SARS-CoV-2 clearance. These patients were characterized by poor humoral immune responses and a compensatory increase in $CD8^+$ T cell activity which was insufficient to achieve viral clearance. Patients who achieved viral clearance despite absent B cell responses exhibited a highly clonal class II-specific $CD4^+$ T cell response. These results are consistent with distinct roles for arms of the adaptive immune system in achieving acute and long-term control of viral infections.

RESULTS

Delayed COVID-19 viral clearance in patients with hematologic malignancies

We performed a prospective observational cohort study of 103 patients with cancer who developed COVID-19 infection with subsequent clinical improvement (Figure 1 and Table S1). All patients had received treatment at Memorial Sloan Kettering Cancer Center (MSKCC). The median age of the cohort was 64 years; 55% were female, 73% were white, and 16% were black (Table 1). Fifty-three percent were current or former smokers. Fifty-two patients had solid cancer; most solid tumor malignancies were lung (66%), followed by breast (6%) and colorectal (6%). Fifty-one patients had hematologic malignancies, including 58% with B cell lymphoma, 12% with chronic lymphocytic leukemia, and 12% with myeloid malignancies. Sixty percent of patients had received cancer-directed therapy within 6 months prior to COVID-19 diagnosis, including B cell-depleting therapy in 41% and PD-1 targeting antibodies in 25%.

All patients had documented SARS-CoV-2 positivity, either by nasopharyngeal swab performed at MSKCC (78%) or outside documentation of PCR positivity (22%) (Figure 1). The majority of patients were also assessed for a humoral immune response to COVID-19 via semi-quantitative IgG antibodies to the nucleocapsid region of the viral proteome (88%). During the course of COVID-19 infection, 62% of patients required hospitalization. Forty-six percent had severe COVID-19 as defined by the Infectious Disease Society of America guidelines (Hanson et al., 2020), 18% required intensive care unit (ICU)-level care, and 14% were intubated. COVID-19-directed therapies included remdesivir in 29%, dexamethasone in 19%, and convalescent plasma in 29%. Despite initial clinical recovery meeting inclusion criteria for convalescent disease, 18% of patients subsequently clinically declined and required readmission for COVID-19-related disease, and 8% of patients in the cohort ultimately died of COVID-19; these patients were included in the analysis based on meeting initial inclusion criteria. Repeat nasopharyngeal swab testing was performed as per the treating clinician's discretion in 42% of patients. Most of these tests were performed for evidence of ongoing clinical symptoms as demonstrated by the strong correlation of duration of symptoms with the number of PCR tests ordered (Figures S1A and S1B). Patients who were deemed to have symptomatically improved by their treating physician and had consented to MSKCC's biobanking protocol (MSKCC IRB #06-107) had their blood drawn for additional research assays described in Figure 1. Patients with hematologic cancers had a longer interval between initial infection and research blood draws, consistent with a higher frequency of prolonged disease; relative to the last known date of PCR positivity, the time to peripheral blood acquisition and research assays was similar between the two groups (Figures S1C–S1F).

Overall, 22% of patients experienced prolonged SARS-CoV-2 positivity, defined as a positive SARS-CoV-2 PCR at least 30 days after initial PCR positivity. Duration of PCR positivity ranged from 0 to 268 days in the overall cohort. Persistent PCR positivity was significantly more frequent in patients with hematologic malignancies, and persistent PCR positivity was significantly associated with subsequent hospitalization because of COVID as well as death attributable to COVID (Figures 2A–2C). Patients with hematologic malignancies, and in particular patients who had received anti-CD20 therapy, had a higher peak viral load, as defined by the number of qPCR cycles required to generate a positive test result (Figure S2A). While patients with solid tumors had a progressive decrease in viral load over time (Figure S2B), patients with hematologic malignancies had both more persistent and significantly greater viral loads, reflected by a longer duration of PCR positivity as well a higher viral load at the first quantitative assessment more than 20 days after initial PCR positivity (Figures 2C, S2B, and S2C). Consistent with this observation, a higher proportion of patients treated with anti-CD20 had prolonged viral PCR positivity (Figure 2C).

To better understand factors contributing to delayed viral clearance in patients with cancer, we first asked whether viral persistence was associated with features of acute infection. We performed integrated correlation mapping of clinical and laboratory assessments obtained within 72 h of primary infection (Figure 2D and Table S1). This analysis revealed several correlations of interest. First, clinical metrics of initial disease severity clustered closely together, including the presence of severe COVID-19, duration of initial hospitalization, and ICU admission (Figure 2D). Similarly, markers of inflammation such as white blood cell count, absolute neutrophil count, and lactate dehydrogenase clustered together. Notably, nucleocapsid and receptor-binding domain (RBD) immunoglobulin G (IgG) titers correlated with higher peak and prolonged viral RT-PCR cycles (lower viral load). Conversely, hematologic malignancy and receipt of B cell-depleting therapy was associated with a higher viral load,

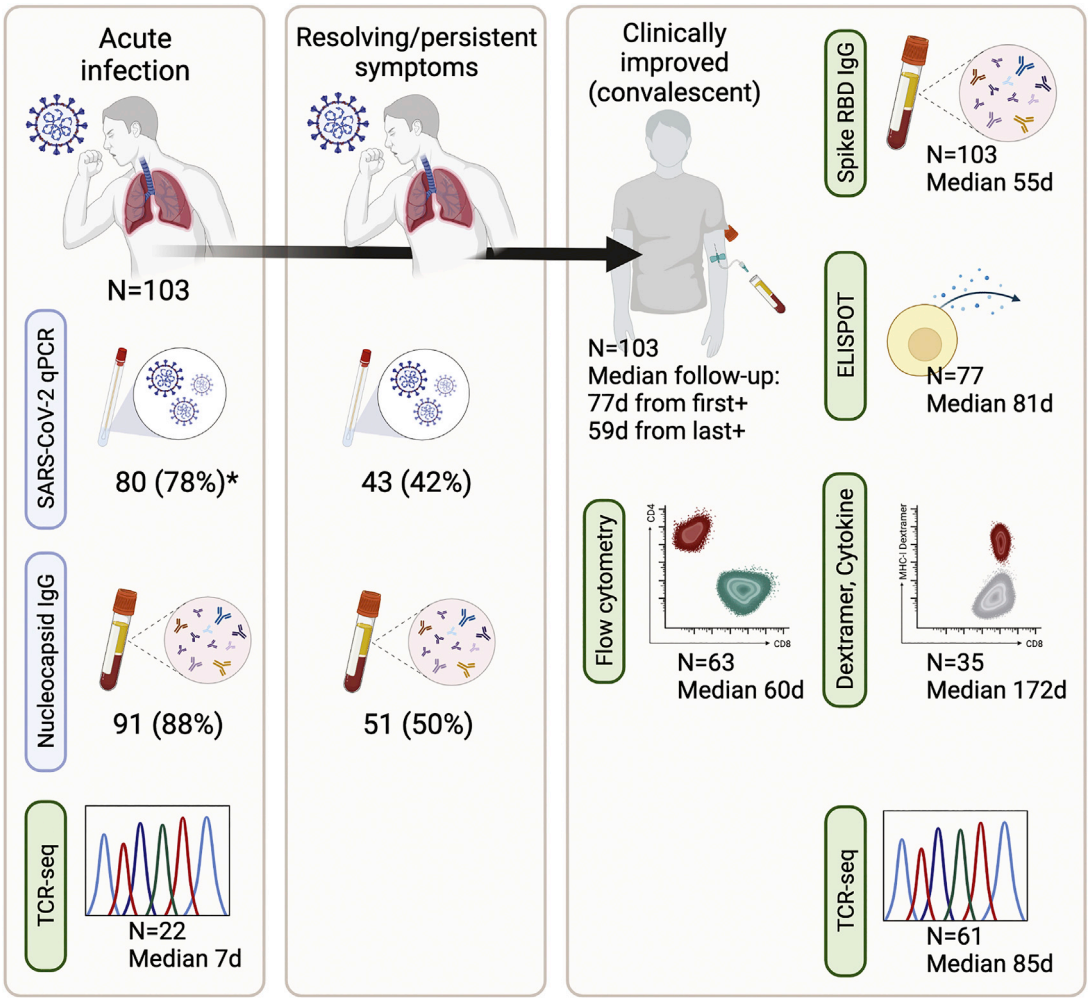

Figure 1. Longitudinal evaluation of patients during and following acute COVID-19

Image depicts workflow for biospecimen acquisition from patients admitted to MSKCC during and following recovery from COVID-19 infection. Number of patients for whom each assay was performed and median time following initial PCR positivity as indicated. See also Table 1 and Figure S1.

suggesting that development of robust humoral immunity is key to viral clearance and that diminished humoral immunity may be the primary driver of impaired viral clearance in this population.

Impaired humoral immunity predisposes patients to persistent SARS-CoV-2 infection

We therefore performed serologic analysis for antibodies targeting the nucleocapsid and the Spike RBD regions of the SARS-CoV-2 proteome (Figure S2D). Only two patients had a positive nucleocapsid IgG titer prior to documented SARS-CoV-2 PCR positivity. All patients achieved peak antibody titers in the first 100 days following documented positivity, reflecting the known kinetics of serum antibodies (Figure 2E). However, patients with hematologic malignancies demonstrated both lower peak and lower sustained antibody titers to both the nucleocapsid and RBD regions (Figures 2E, 2F, and S2E), which was largely driven by patients with lymphoid malignancies (Figure S2F). Consistent with published data (Lee et al., 2022), B cell depletion was strongly associated with prolonged viremia, independent of infection-driven lymphopenia (Figure S2G). Of note, the nucleocapsid index did not correlate with peak viral load during the acute phase of the disease. Rather, there was a strong correlation between nucleocapsid index and the viral load during prolonged disease (prolonged viral load) (Figures 2G, 2H, and S2H). These data suggest that although antibody responses may not have an immediate impact on viral load, they are critical for eventual viral clearance.

We next asked whether humoral responses to infection in cancer patients varied according to clinical parameters known to be associated with outcomes to COVID-19 infection. Consistent with prior reports in cancer-free populations, older age, female gender, and hospitalization were associated with higher antibody titers in patients with solid tumors (Figures S2I–S2K) (Zeng et al., 2021). However, patients with hematologic malignancies did not show increased antibody titers in any of these

Table 1. Demographic and outcome data for previously COVID-positive patients at MSKCC

	Solid		Heme	
	Number	%	Number	%
	52	50.5	51	49.5
Age (years)	65.8 (28–87)		61 (36–85)	
Female	30	57.7	28	54.9
White	36	69.2	39	76.5
Cardiac disease	36	69.2	19	37.3
Pulmonary disease	39	75	7	13.7
Diabetes	18	34.6	12	23.5
BMI	27.5		28.4	
Smoking	32	61.5	23	45.1
Anti-PD-1	13	25		
Anti-CD20			21	41.2
Hospitalized	31	59.6	33	64.7
Severe disease	23	44.2	25	49
ICU	6	11.5	13	25.5
≥14 days hospitalization	15	28.8	14	27.5
≥30 days PCR	4	7.7	19	37.3

populations, nor did they have increased antibody titers over time during prolonged infection (Figures S2I–S2M).

Taken together, these data suggest that a loss of humoral immunity is a significant contributor to the risk of impaired SARS-CoV-2 clearance observed in patients with hematologic malignancies. To determine whether this humoral defect could also be observed on a cellular level, we analyzed peripheral blood B cell immunophenotypes in the peripheral blood of patients who had clinically recovered from prior COVID-19 infection. Viral persistence was not associated with the frequency of the total B cell pool ($CD19^+/CD20^+$), class-switched memory B cells ($CD27^+/IgD^-$), circulating plasmablasts ($CD27^+/CD38^+$), or proliferating non-naive B cells ($IgD^-/Ki\text{-}67^+$) (Figures S2N and S2O). When we assessed the relationship between B cell counts in the peripheral blood and nucleocapsid IgG levels, we found that solid tumor patients with minimal circulating levels of B cells still tended to generally produce robust nucleocapsid IgG, while in patients with hematologic malignancies IgG production seemed to be largely restricted to either patients with adequate B cell counts or patients who had received convalescent plasma (Figure S2P). Furthermore, some patients with hematologic malignancies did not produce nucleocapsid IgG despite adequate B cell counts. These results suggest that suppression of humoral immunity in patients with prolonged COVID-19 PCR positivity is not attributable to purely quantitative and qualitative B cell defects in patients with hematologic malignancies. Rather, the etiology of suppressed humoral immunity is likely heterogeneous, influenced by several patient-associated variables including cancer type, cancer treatment, and COVID-19 treatment, among others.

Altered $CD8^+$ T cell differentiation in hematologic cancer patients with prolonged SARS-CoV-2 PCR positivity

While lack of a sufficient humoral immune response was associated with impaired viral clearance, ultimately most patients with cancer recovered from COVID-19, including those who had received B cell-directed therapies. This raised two key biological questions: how are B cell-depleted patients able to recover from COVID-19, and which immunological features are predictive of viral persistence in B cell-depleted patients? To investigate the cellular responses that might potentially compensate for deficient humoral immunity in COVID-19, we performed high-dimensional analysis of lymphocytes from 63 patients who had recovered from COVID-19 using 27-parameter flow cytometry (Figure 3A). We used the earth mover's distance (EMD) metric to calculate the distance between uniform manifold approximation and projections (UMAPs) for every pair of patients. Clustering on EMD values identified four major groups of patients distinguished by both the distribution and phenotype of cell subtypes (Figure 3B). A fifth distinct group had only two patients. UMAP representation of the 27-parameter flow-cytometry data highlighted discrete islands of B cells, $CD4^+$ T cells, and $CD8^+$ T cells (Figure 3C). EMD group 1 was defined by B cell depletion and a CD8-dominant T cell response. Group 2 was defined by B cell depletion and a CD4-dominant T cell response. Group 3 exhibited balanced levels of CD4, CD8, and B cells. Finally, group 4 had balanced CD4 and CD8 T cell responses in the setting of B cell depletion (Figure S3A). While groups 1, 2, and 4 were B cell depleted, we did not observe any difference in peak viral load, hospitalization rate, overall white blood cell counts, or inflammatory markers between EMD groups (Figures S3B–S3D). Notably, patients with prolonged PCR positivity were enriched in group 1, which was characterized by B cell depletion but intact $CD8^+$ T cell counts (Figure 3D and Table S2). More broadly, patients with hematologic cancer and prolonged disease had a gain in CD8-associated UMAP regions and a higher frequency of $CD8^+$ T cells compared with either hematologic malignancy patients without prolonged disease or patients with solid cancers (Figures 3E and 3F).

To understand whether persistent viral infection altered the global phenotype of peripheral blood $CD8^+$ T cells, we performed UMAP representation of $CD8^+$ T cells (Figure 3G). FlowSOM clustering revealed ten cell clusters with distinct immunophenotypes (Figure 3H). Comparison of EMD groups revealed that group 1, which was characterized by B cell depletion and high levels of $CD8^+$ T cells, had very low proportions of central memory T cells (cluster 9, $CD27^+$/CCR7-med/$CD45RA^-$/TCF-1-high) and naive T cells (cluster 10, $CD27^+/CD45RA^+$/CCR7-high) but high proportions of terminally differentiated effector memory $CD8^+$ T cells (Temra) (cluster 2, $CD27^-$/$CD45RA^+$/$CX3CR1^+$/T-bet-high) (Figures 3I and 3J). We therefore asked whether a shift from a central memory phenotype to a terminally differentiated effector memory phenotype was characteristic of prolonged PCR positivity. Indeed, patients with prolonged disease exhibited a significant decrease in central memory T cells and an increase in Temra (Figures 3K–3L). Thus, prolonged SARS-CoV-2 infection is associated with increased effector $CD8^+$ T cell differentiation at the expense of memory $CD8^+$ T cell differentiation.

Persistent functional T cell responses in patients with hematologic malignancies with delayed SARS-CoV-2 clearance

We previously reported that CD8 T cell responses significantly contribute to survival during acute COVID-19 infection (Bange

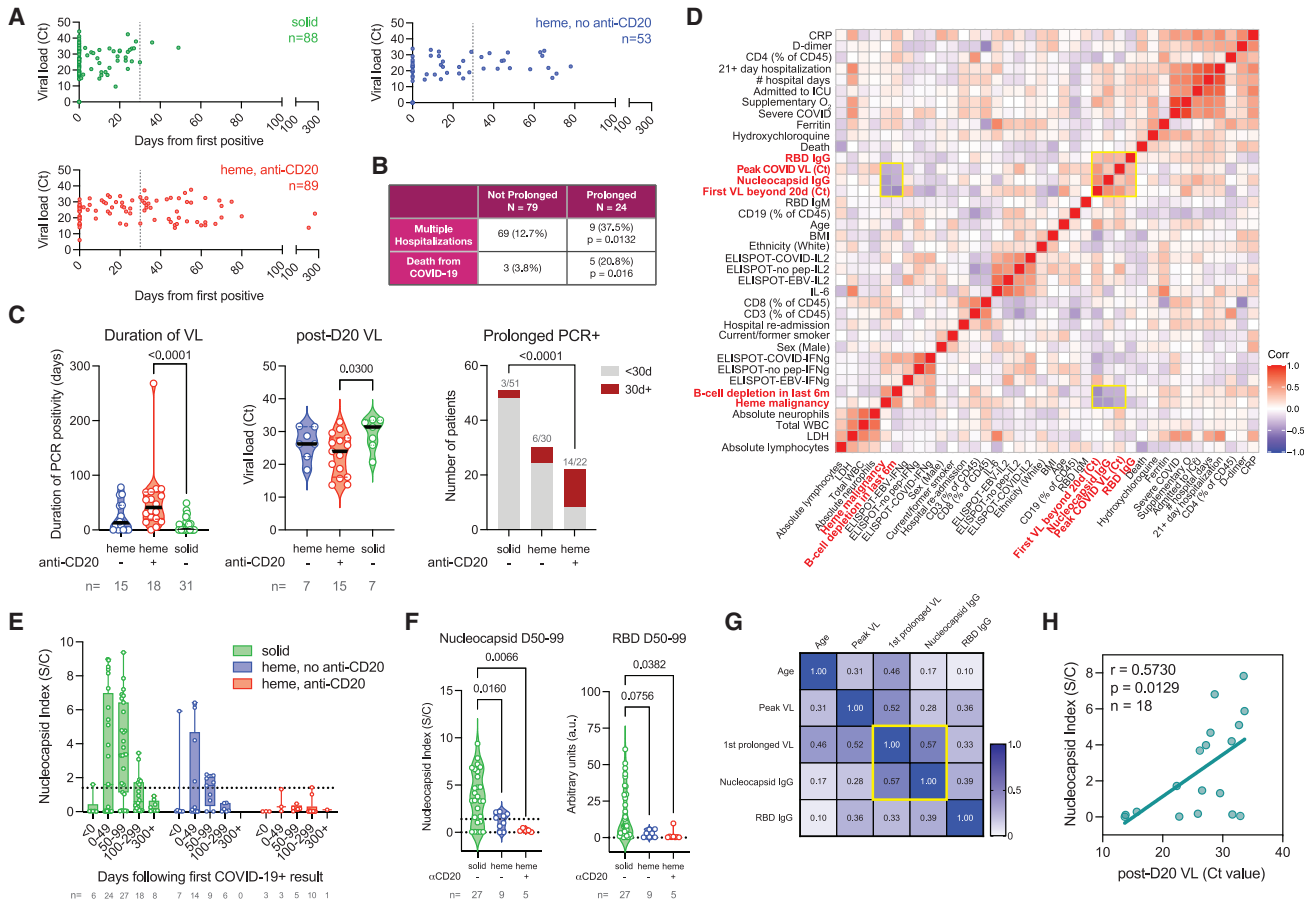

Figure 2. Impaired humoral immunity in cancer patients with delayed SARS-CoV-2 clearance

(A) SARS-CoV-2 viral RT-PCR counts in patients, normalized to the date of first positive test. Dashed line depicts 30-day cutoff for prolonged PCR positivity.

(B) Risk of rehospitalization and ultimate death from COVID-19 in patients with or without prolonged PCR positivity during initial infection.

(C) Left: duration of PCR positivity in patients with more than one positive PCR test. Center: median viral RT-PCR count in first positive PCR test more than 20 days after initial positive test. Right: proportion of patients with prolonged PCR positivity.

(D) Spearman correlation and hierarchical clustering of indicated clinical and laboratory features for previously COVID-19-positive cancer patients.

(E) Nucleocapsid index over time normalized to first positive COVID-19 PCR test, stratified by malignancy and B cell-depleting therapy.

(F) Nucleocapsid index (left) and RBD IgG titer (right) for patients 50–99 days following initial COVID-19 PCR positivity (E).

(G) Spearman correlation and hierarchical clustering of clinical and laboratory factors most closely associated with prolonged PCR positivity. R value for each correlation as indicated.

(H) Correlation of nucleocapsid index with first viral RT-PCR value more than 20 days following initial PCR positivity.

p values calculated using independent two-sample t test. See also Figure S2 and Table S1.

et al., 2021). While B cell depletion is associated with prolonged and/or recurrent COVID-19 infection, the majority of B cell-depleted patients successfully recover (Lee et al., 2022). To test whether our observed increase in Temra in patients with prolonged PCR positivity reflected ongoing partial compensation by CD8 T cells, we evaluated functional T cell responses to SARS-CoV-2 antigens in previously COVID-19 patients a median of 81 days following initial infection (Figure 4A). Peripheral blood mononuclear cells (PBMCs) were stimulated for 18 h with a SARS-CoV-2 select peptide pool containing class I- and II-restricted peptides derived from the entire proteome of SARS-CoV-2. Virus-specific responses were assessed by interferon-γ (IFN-γ) and interleukin-2 (IL-2) ELISpot assays and compared with controls with no peptides or stimulated with a standard Epstein-Barr virus (EBV) peptide pool (Figure 4A). On integrated correlation mapping, peptide-specific T cell IFN-γ responses were associated with hematologic cancer and B cell depletion along with chronically elevated viral load, while T cell IFN-γ responses were anticorrelated with nucleocapsid IgG titer (Figure 4B), suggesting that functional T cell responses were in fact enhanced in patients with B cell depletion and/or prolonged disease. Consistently, we found that while no association of COVID-specific T cell responses with age, gender, or hospitalization was observed (Figures S4A–S4C), patients with hematologic malignancies had greater SARS-CoV-2-specific functional T cell responses compared with patients with solid tumor malignancies (Figure S4D). This increased functional response persisted and was most significant at 50–99 days following initial COVID-19 infection (Figure 4C). Patients with prolonged viremia had the greatest magnitude of SARS-CoV-2-specific T cell

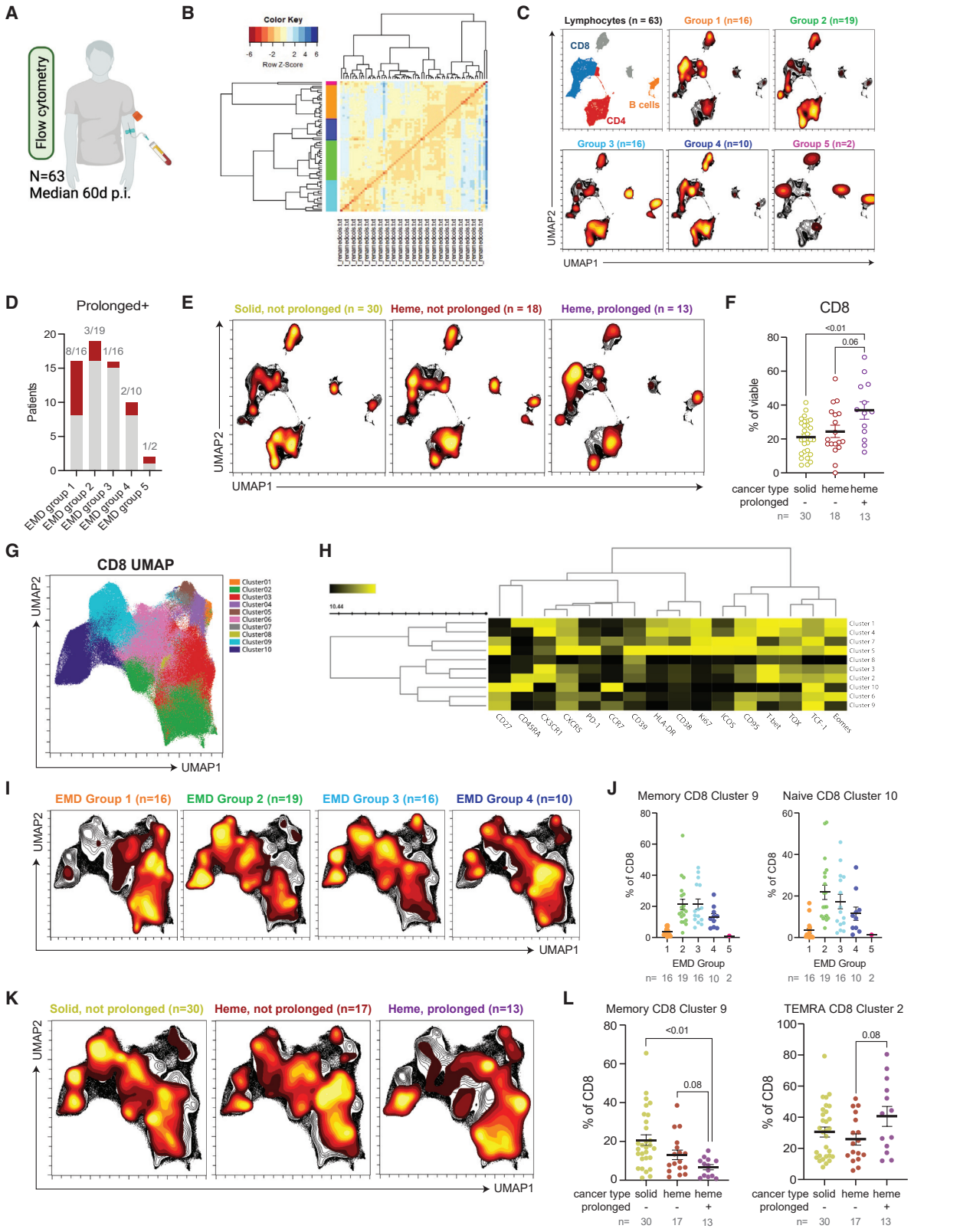

Figure 3. Robust CD8⁺ T cell responses but impaired memory transition in cancer patients with prolonged COVID-19

(A) Number of patient PBMCs on which multi-parametric flow cytometry was performed, and median time following initial PCR positivity of flow-cytometry samples.

(legend continued on next page)

responses compared with hematologic and solid cancer patients who recovered (Figure 4D), suggesting that enhanced functional T cell responses in patients with hematologic malignancy are driven by prolonged infection, but not sufficiently enough for viral clearance. The most robust SARS-CoV-2-specific T cell responses were observed in patients with indolent lymphoid malignancies (Figure S4E). This may be due to the fact that patients with indolent lymphoma were more likely to be treated with B cell-targeted therapies (anti-CD20, Bruton tyrosine kinase inhibitor, chimeric antigen receptor T cell) alone (9 of 18, 50%) as compared with patients with aggressive lymphomas (4 of 19, 21%) or myeloid neoplasms (1 of 6, 17%), whereas chemotherapy was more common in patients with aggressive lymphomas (14 of 19, 74%) and myeloid neoplasms (5 of /6, 83%) as compared with patients with indolent lymphomas (7/18, 39%). Consistent with this, receipt of B cell-targeting agents, but not chemotherapy, was associated with increased peptide-specific IFN-γ responses in patients with hematologic malignancies (Figure 4E).

Interestingly, COVID peptide-specific IL-2 responses did not display the same pattern as peptide-specific IFN-γ responses in this patient population. Integrated correlation mapping did not show any association between peptide-specific IL-2 responses and either prolonged viremia or B cell depletion (Figure 4B). Consistent with this lack of association, peptide-specific IL-2 production was only mildly and non-significantly increased in patients with hematologic malignancies (Figures S4F and S4G), and we did not observe any persistent enhancement of peptide-specific IL-2 production over time (Figure S4H), nor did patients with prolonged disease or patients who had received B cell-depleting therapies exhibit an enhanced peptide-specific IL-2 response (Figures S4I and S4J). Given that IL-2 is produced primarily, though not exclusively, by activated $CD4^+$ T cells (Malek, 2008), these results suggested that compensatory T cell immunity in B cell-depleted patients following COVID infection might be driven by IFN-γ secreting CD8 T cells. Indeed, when we performed SARS-CoV-2 peptide stimulation in conjunction with intracellular cytokine staining, SARS-CoV-2 IFN-γ ELISpot responses correlated with the percentage of intracellular IFN-γ in CD8 T cells. (Figures 4F and S4K). Moreover, SARS-CoV-2 IFN-γ ELISpot responses correlated with the frequency of activated ($HLA\text{-}DR^+CD38^+$) SARS-CoV-2-specific CD8 T cells as identified by class 1 major histocompatibility complex (MHC)-peptide dextramers (Figure 4G). Altogether, these data support the fact that patients with hematologic cancer and prolonged SARS-CoV-2 infection exhibit robust ongoing antigen-specific CD8 T cell responses.

Broad but poorly converged clonal $CD8^+$ T cell responses in B cell-depleted patients with prolonged SARS-CoV-2 infections

We next sought to understand the impact of prolonged viremia on the SARS-CoV-2-specific T cell repertoire. We therefore performed bulk T cell receptor (TCR) sequencing and identified putative COVID-19 associated MHC class I- and class II-specific T cell clones in 26 samples with active infection, defined as samples with symptomatic COVID-19 infection in the context of a recent positive PCR swab (22 patients, median 7 days post infection), and 95 convalescent samples, defined as samples taken after the patient had clinically recovered from a prior documented COVID-19 infection (61 patients, median of 85 days post infection, including 14 patients with prolonged disease) (Figure 5A). We leveraged the immunoSEQ T-MAP database generated using the multiplex identification of TCR antigen assay (Klinger et al., 2015; Snyder et al., 2020; Mudd et al., 2022), which provided a library of putative COVID-19-peptide-specific $CD8^+$ and $CD4^+$ T cell responses. We focused initially on class I-reactive COVID TCRs given our flow cytometry and functional data suggesting persistent $CD8^+$ T cell activity in patients with prolonged PCR positivity. Overall, we identified 41,082 COVID-19-associated TCRs in our cohort, which overlapped with those found to expand in an MHC-I-restricted fashion in the COVID-19 T-MAP database. The identified TCRs mapped to antigens from across the SARS-CoV-2 proteome, including epitopes derived from protein S, ORF1ab, and ORF7b (Figure 5B), and included private as well as shared SARS-CoV-2-associated clonotypes. TCR responses to the 219 most commonly targeted antigens were present in TCR repertoires of all 69 patients.

Stratification of TCR responses across the viral genome by HLA type did not reveal differences in TCR response patterns based on distinct HLA presentation patterns (Table S3). Moreover, the 26 partially overlapping dominant peptides were predicted to bind 42 out of 49 HLA A, B, and C alleles present in this cohort and for which NetMHC4.0 (Andreatta and Nielsen,

(B) Hierarchical clustering of earth mover's distance (EMD) using Pearson's correlation of high-dimensional flow-cytometry data from all patients, calculated pairwise for lymphocyte populations.
(C) Uniform manifold approximation and projection (UMAP) of concatenated lymphocyte populations for each EMD group (yellow, high density; black, low density).
(D) Prolonged PCR positivity, stratified by EMD group.
(E) UMAP projections of concatenated lymphocyte populations for cancer patients stratified by malignancy subtype and the presence or absence of prolonged disease.
(F) Quantitation of CD8 T cell frequencies in cancer patients stratified by malignancy subtype and the presence or absence of prolonged disease.
(G) UMAP projection of CD8 T cell clusters identified by FlowSOM.
(H) Heatmap showing expression patterns of various markers, stratified by FlowSOM CD8 T cell cluster. Heat scale calculated as column *Z* score of mean fluorescence intensity.
(I) UMAP projections of concatenated CD8 T cell populations for cancer patients stratified by EMD group.
(J) Quantitation of memory (cluster 9) and naive (cluster 10) CD8 T cell frequencies in cancer patients stratified by EMD group.
(K) UMAP projections of concatenated CD8 T cell populations for cancer patients stratified by malignancy subtype and the presence or absence of prolonged disease.
(L) Quantitation of memory (cluster 9) and short-lived effector (Temra, cluster 2) CD8 T cell frequencies in cancer patients stratified by malignancy subtype and the presence or absence of prolonged disease.
p values calculated using independent two-sample t test. See also Figure S3 and Table S2.

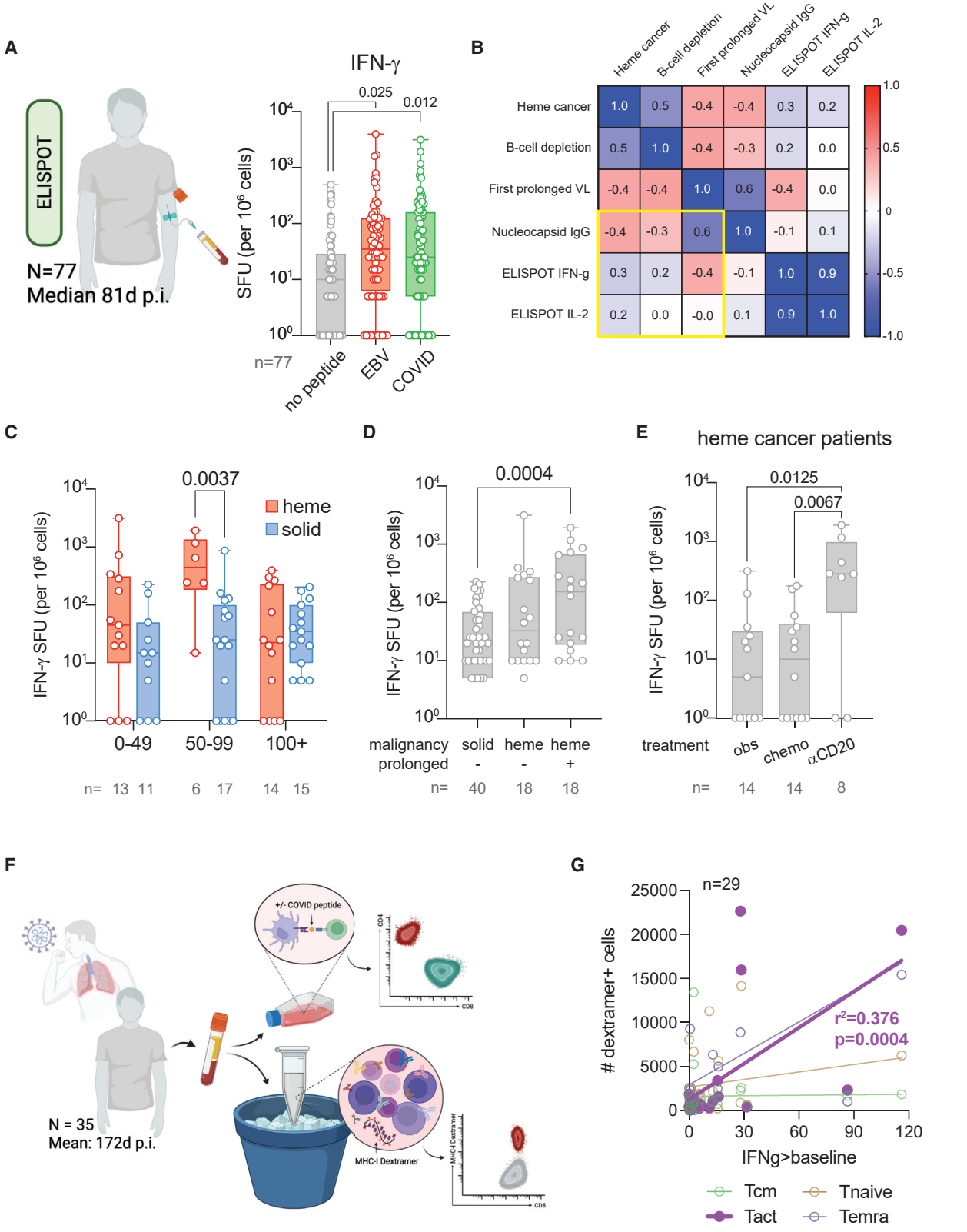

Figure 4. Prolonged COVID-19 triggers ongoing, class I-specific IFN-γ responses in hematologic cancer patients

(A) Left: number of patient PBMCs on which ELISpot assays were performed, and median time following initial PCR positivity of ELISpot samples. Right: increase in IFN-γ production following PBMC culture for 18 h in the presence of indicated peptides.

(legend continued on next page)

2016) binding predictions are available, suggesting that these dominant peptides are able to be presented widely by this patient population. Overall, our results are indicative of a broad CD8$^+$ T cell response to native COVID-19 infection whose heterogeneity is not influenced by HLA background.

We first asked how SARS-CoV-2-associated clonotypes evolved as patients transitioned from acute infection to clinical recovery by evaluating their clonal breadth (number of unique TCR rearrangements), depth (overall frequency of specific TCRs), and convergence (representing generation of different nucleotide TCR sequences, TCRs with convergent amino acid sequence and, therefore, shared antigen specificity). During a conventional CD8$^+$ T cell response, clonal breadth and depth expand at early time points after antigen exposure. As the infectious agent is cleared, transition to T cell memory is marked by clonal contraction as well as an increase in TCR convergence, indicative of selection for high-affinity TCR clones. We binned samples from COVID-19-infected individuals by days following COVID-19 positivity, coded them by whether patients were actively infected or recovered, and compared clonal dynamics with a set of 666 samples from patients and healthy donors without evidence of prior COVID-19 infection (Emerson et al., 2017). The breadth and clonality of class I SARS-CoV-2-associated TCRs were higher in both acutely infected and convalescent individuals compared with the control group of healthy donors and cytomegalovirus patients whose TCR repertoires were sequenced prior to the COVID-19 pandemic (Figures 5C and S5A). COVID-specific TCR breadth increased over time, peaking on days 8–14 after the first positive COVID test and slightly decreasing to a level still above the baseline. Clonality of class I COVID-19 associated TCRs also increased over time, peaking at weeks 7–8 after the first positive COVID test.

Next, we asked whether SARS-CoV-2-associated CD8$^+$ TCR dynamics varied between patients with prolonged disease and those with successful viral clearance. Patients with efficient viral clearance exhibited a decrease in SARS-CoV-2-associated class I TCR breadth, as expected following antigen clearance (Figures 5D and 5E) while SARS-CoV-2-associated TCR breadth continued to increase in patients with prolonged PCR positivity (Figures 5D and 5E). These changes were not seen in a control set of irrelevant class I-specific TCRs (Figure 5E, VDJDB). The increase in TCR breadth was accompanied by an increase in TCR clonality but not TCR depth (Figures S5B and S5C). To further confirm that these changes in the breadth of TCR repertoire were relevant to active SARS-CoV-2-specific CD8 T cells, we tested the association between SARS-CoV-2-specific TCR breadth and SARS-CoV-2 dextramer$^+$ CD8 T cells. Indeed, there was a greater frequency of activated SARS-CoV-2 dextramer$^+$ CD8 T cells in patients with prolonged disease (Figure 5F). Moreover, SARS-CoV-2-specific TCR breadth was associated with activated (HLA-DR$^+$CD38$^+$) but not naive or memory dextramer$^+$ CD8 T cells (Figure 5G) while TCR clonality inversely correlated only with naive T cells (Figure S5D). Taken together, these results are consistent with ongoing engagement of a broad set of SARS-CoV-2-reactive CD8$^+$ T cells due to viral persistence.

We next asked whether our observed differences in TCR clonality in patients with prolonged disease were linked to differences in their underlying activation and differentiation state. For 50 patients with TCR sequencing and immunophenotype-based EMD cluster assignment, we analyzed TCR metrics according to EMD groups based on global peripheral blood immune phenotypes. In EMD group 1, which is characterized by increased effector CD8$^+$ T cell differentiation and diminished memory differentiation in the setting of B cell depletion, we observed an increased breadth and clonality of SARS-CoV-2 reactive class I-specific TCRs. However, patients in this group did not show an increase in class I-specific clonal depth and exhibited significantly decreased convergence (Figures 5H, S5E, and S5F). Within EMD group 1, patients with prolonged disease exhibited the highest breadth but lowest convergence and clonality (Figures S5G and S5H). Conversely, EMD group 2, which is also characterized by B cell depletion but demonstrated normal CD8$^+$ T cell memory development, exhibited a relatively narrow COVID-specific MHC-I-reactive TCR breadth but significantly higher convergence compared with patients in group 1. TCR convergence, or homogenization, occurs during selection of high-affinity antigen-specific clones during the transition to T cell memory (Kedzierska et al., 2008). Thus, in the setting of prolonged disease, there would be an expansion of the SARS-CoV-2-reactive TCR repertoire but a lack of competitive selection for high-affinity TCR clones characteristic of the transition to CD8$^+$ T cell memory. Consistent with this hypothesis, patients with prolonged disease had significantly lower TCR convergence (Figure 5I), such that significantly fewer patients with prolonged disease (2 of 14, 14%) exhibited a narrow and converged COVID-associated class I-specific TCR repertoire as compared with patients without prolonged disease (26 of 55, 47%) (Figure S5I). Altogether, these results are consistent with a robust effector CD8 T cell response and continual recruitment of SARS-CoV-2-specific CD8 T cells in the setting of persistent viral load.

Enhanced CD4$^+$ T cell immunity in B cell-depleted patients with preserved SARS-CoV-2 clearance

Despite increased functional CD8$^+$ T cell responses in patients with B cell depletion, EMD group 1, which was marked by CD8$^+$ T cell dominance, had the highest level of SARS-CoV-2 persistence, while EMD group 2, which was marked by CD4$^+$

(B) Spearman's correlation and hierarchical clustering of clinical and laboratory factors associated with prolonged PCR positivity and antibody responses. R value for each correlation as indicated.
(C) COVID peptide-specific IFN-γ spot-forming units (SFU) in samples obtained at the indicated times following first documented COVID PCR positivity.
(D and E) COVID peptide-specific IFN-γ SFU in patients based on prolonged PCR positivity (D) or active treatment subtype (E).
(F) Number of patient PBMCs and median time following initial PCR positivity for which SARS-CoV-2 class I dextramer staining and flow-cytometry-based restimulation assays were performed.
(G) SARS-CoV-2 class I dextramer-specific activated CD8$^+$ T cells, but not naive, central memory, or Temra cells correlated with IFN-γ release as measured by ELISpot.
p values calculated using independent two-sample t test. See also Figure S4.

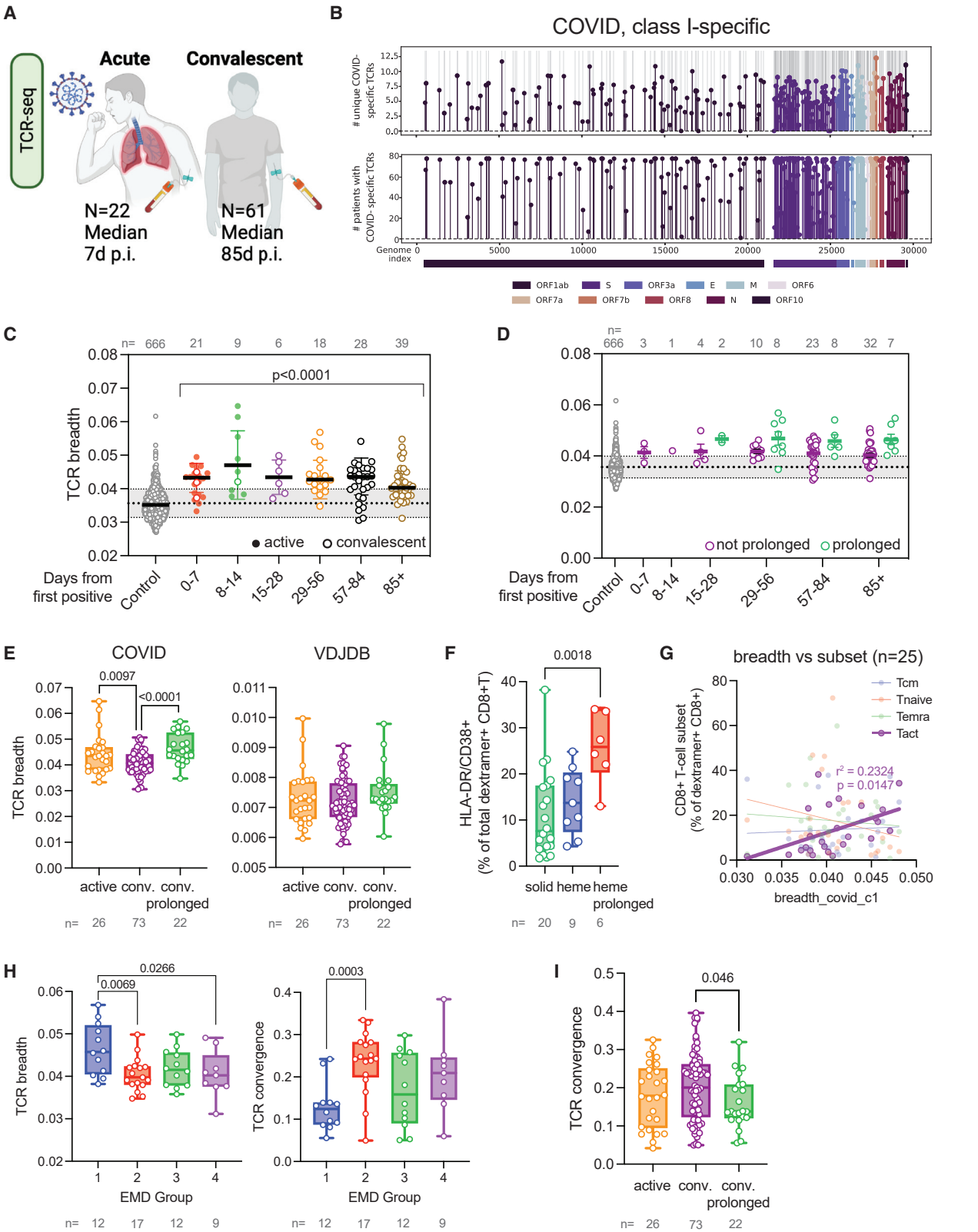

Figure 5. Prolonged COVID positivity is characterized by broad but poorly expanded and selected antigen-specific CD8⁺ T cell clones

(A) Summary of samples with bulk TCR sequencing performed. d p.i., days post infection, calculated as number of days between the date when the blood sample was taken for TCR sequencing minus the date of the first positive COVID-19 PCT test.

(legend continued on next page)

T cell dominance, had a much lower incidence of viral persistence despite B cell depletion. We therefore asked whether either EMD groups or patients with persistent PCR positivity exhibited differences in $CD4^+$ T cell differentiation or function. FlowSOM clustering of $CD4^+$ T cells revealed ten cell clusters with distinct immunophenotypes (Figures S6A and S6B). Comparison of EMD groups revealed that group 1, which was characterized by B cell depletion and high levels of $CD8^+$ T cells, also had high proportions of terminal effector-like $CD4^+$ T cells ($CD45RA^-$, $CCR7^-$, T-bet^+, PD-1^+, Ki-67-low, CX3CR1-high) (Figures S6C and S6D); however, an increase in these cells was not uniformly seen in all patients with prolonged disease (Figures S6E and S6F).

We then asked whether the relatively poor viral control among patients in EMD group 1 could be attributed to functional defects in $CD4^+$ T cell responses within this subgroup. Analysis of cytokine production following peptide stimulation revealed that among EMD groups lacking B cells, patients in EMD group 1 had the lowest frequency of COVID-specific IL-2 production, whereas patients in EMD groups 2 and 4, whose $CD4^+$ T cells were maintained in the absence of B cells, produced higher levels of COVID-specific IL-2, consistent with a dominant role for $CD4^+$ T cells in the production of this cytokine (Figure S6G) (Pfizenmaier et al., 1984; Tham and Mescher, 2002).

To further probe whether patients in group 1 had evidence of a less potent COVID-specific $CD4^+$ T cell response, we curated TCR-sequencing data from convalescent patients to focus on COVID-reactive, MHC class II-specific TCRs. We identified 1,918 COVID-19-associated TCRs found to expand in an MHC-II-restricted fashion in the T-MAP COVID database (see STAR Methods). The identified TCRs mapped to antigens from across the viral proteome (Figure 6A), with the exception of genes ORF1ab and ORF10, epitopes not included in the T-MAP COVID database. Shared immune responses, whereby multiple patients share the same COVID-19-associated TCR clone, were observed predominantly for genes S, N, M, and ORF3a. TCRs associated with the ten most commonly targeted class II epitopes were present in TCR repertoires of all 69 patients.

Similar to our analysis of $CD8^+$ T cell clones over time, we binned samples from previously COVID-19-infected individuals by days following initial COVID positivity and compared clonal dynamics with a set of 666 patients and healthy donors without evidence of prior COVID infection (Emerson et al., 2017). The breadth of COVID-19 class II-specific TCRs followed a similar dynamic, increasing over time and peaking at days 15–28 from the first positive COVID-19 PCR test, then decreasing slightly but remaining above that of the pre-COVID-19 control group (Figure 6B). Clonality of COVID-19 class II-specific TCRs did not change significantly over time (Figure S6H).

We next asked whether differences in class II-specific TCR patterns were associated with patient characteristics, COVID outcomes, or peripheral blood immunophenotypes. Patients with prolonged PCR positivity demonstrated increased class II-specific TCR breadth as compared with patients without prolonged disease (Figure S6I), but without any change in TCR clonality, depth, or convergence to suggest antigen-specific expansion or selection of class II-specific TCRs (Figures S6J–S6L). Given the significant role of B cells in enabling viral clearance, we focused our analysis on the three EMD groups with absent B cell responses (EMD groups 1, 2, and 4) (Figure 6C). Consistent with our functional ELISpot data, we found that patients in EMD group 1 exhibited broad but poorly expanded COVID MHC-II-specific TCRs with low convergence (Figures 6D–6G). Conversely, EMD group 2 demonstrated a narrow but highly expanded and converged COVID-reactive, class II-specific TCR landscape, indicative of competitive selection of COVID-reactive class II-specific $CD4^+$ T cell clones. EMD group 4, which exhibited a balanced CD4 and CD8 T cell response in the absence of B cells, had a class II-specific TCR breadth, depth, and convergence that was between EMD groups 1 and 2. Taken together, these data suggest that antigen-specific $CD4^+$ T cell responses play a role in efficient SARS-CoV-2 viral clearance, particularly in the absence of B cell function.

DISCUSSION

An ongoing concern during the COVID-19 pandemic is the poor outcomes experienced by patients with comorbid diseases, and in particular patients with cancer. Dedicated studies in this patient population have revealed notable similarities, as well as key distinctions, in clinical and immunological risk factors for poor outcomes during acute COVID-19 infection. For example, elevated acute phase reactants, including IL-6 and C-reactive

(B) Distribution of COVID-19 class I-specific TCRs along the SARS-CoV-2 genome. Top: number of unique TCRs associated with an epitope at a specific genomic position across all patients, with gray lines indicating all class I epitopes reported in the T-MAP COVID database. Bottom: number of patients whose TCR repertoires include at least one TCR associated with an epitope at that genomic location.
(C) Breadth of COVID-19 class I-associated TCRs in COVID-19 samples grouped by time from the first positive PCR test compared with a control group of pre-COVID-19 TCR-sequencing samples (Emerson et al., 2017). Dashed line represents the median of the control group, and the gray lane represents median ± 1 SD of the control group. Active samples are represented by filled circles and convalescent samples by open circles. p values were measured by unpaired t test.
(D) Breadth of COVID-19 class I-associated TCRs in COVID-19 samples from convalescent patients, stratified by the presence or absence of prolonged disease.
(E) Breadth of COVID-19 class I-specific TCRs (left) and other known antigen-associated TCRs from the VDJDB dataset (see STAR Methods) (right) in patients with acute COVID-19 infection and in convalescent patients, stratified by the presence or absence of prolonged PCR positivity. One TCR-sequencing sample per patient representing the last available time point was used for this and subsequent analysis of TCR statistics.
(F) Fraction of COVID class I-specific dextramer-positive $CD8^+$ T cells with an activated ($CD38^+$/HLA-DR^+) phenotype in convalescent patients, stratified by malignancy subtype and presence or absence of prolonged PCR positivity.
(G) SARS-CoV-2 class I dextramer-specific activated $CD8^+$ T cells, but not naive, central memory, or Temra cells correlated with putative SARS-CoV-2 class I-specific TCR breadth according to the T-MAP COVID database.
(H) Breadth and convergence of COVID-19 class I-associated TCRs in TCR repertoires of patients in each EMD group.
(I) Convergence of COVID-19 class I-specific TCRs in samples stratified by malignancy subtype and presence or absence of prolonged PCR positivity.
p values calculated using independent two-sample t test. See also Figure S5 and Table S3.

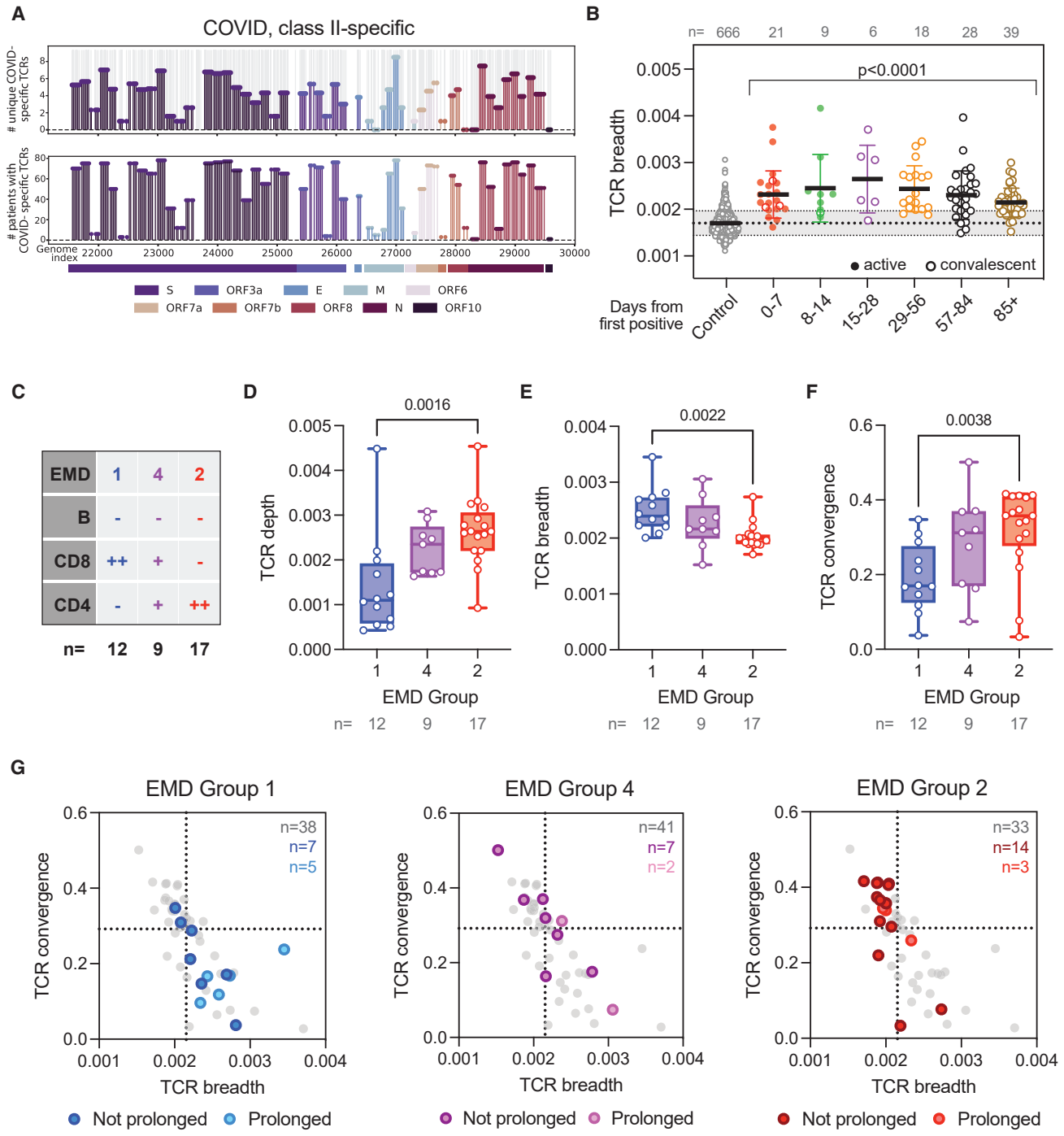

Figure 6. Enhanced antigen-specific CD4⁺ T cell responses contribute to viral clearance in B cell-depleted patients

(A) Distribution of COVID-19 class II-specific TCRs along the SARS-CoV-2 genome. Top: number of unique TCRs associated with an epitope at a specific genomic position across all patients, with gray lines indicating all class I epitopes reported in the T-MAP COVID database. Areas of similar TCR coverage result from overlapping epitopes associated with overlapping sets of associated TCRs. Bottom: number of patients whose TCR repertoires include at least one TCR associated with an epitope at that genomic location.

(B) Breadth of COVID-19 class II-associated TCRs in COVID-19 samples grouped by time from the first positive PCR test compared with the control group of pre-COVID-19 TCR-sequencing samples. Dashed line represents the median of the control group, and the gray lane represents median ± 1 SD of the control group. Stars indicate statistical significance of difference compared with the control, as measured by unpaired t test.

(C) Summary of patient immunophenotypes included in EMD groups 1, 2, and 4. B, B cell depleted; CD8, relative CD8 T cell frequency; CD4, relative CD4 T cell frequency.

(legend continued on next page)

protein, were both observed in patients with and without cancer (Albiges et al., 2020; Chen et al., 2020; Laing et al., 2020). Conversely, while both highly activated $CD8^+$ T cells and robust antibody responses were associated with severe COVID-19 in immunocompetent patients without cancer (Mathew et al., 2020), recent studies have found adaptive immunosuppression, and in particular loss of $CD8^+$ T cell immunity, to be a stronger indicator of poor outcomes in patients with cancer (Bange et al., 2021). Further contributing to morbidity in this population is the inability to achieve durable viral clearance. Persistent COVID-19 infection has been described in patients with hematologic malignancies, and a recent study identified B cell depletion as the dominant risk factor for persistent clinically symptomatic COVID-19 infection (Lee et al., 2022). How patients who lack functional humoral immunity achieve viral clearance is of marked importance given the emergence of variants with partial or complete resistance to antibody-mediated neutralization, as well as descriptions of intrahost viral evolution in patients unable to achieve viral clearance (Choi et al., 2020; Hoffmann et al., 2021; Planas et al., 2021; Wang et al., 2021). We speculated distinct arms of the adaptive immune response might be required for acute viral control and efficient viral clearance in COVID-19-infected patients with cancer, and that exploring compensatory strategies in patients with impaired humoral immunity might provide insights into how durable viral control is achieved.

CD8 T cells play a critical role in early viral control and clinical recovery (Bange et al., 2021). In this article, we establish key roles for B and $CD4^+$ T cell immunity in enabling viral clearance and convalescence from COVID-19 infection. First, we establish loss of humoral immunity as the primary driver of delayed viral clearance in COVID-19-infected patients with cancer. Compared with patients with solid tumors, in whom delayed viral clearance was only observed in 8% (4/52) of patients, prolonged PCR positivity was observed in 37% (19/51) of patients with hematologic malignancies and 62% (13/21) of patients who had received B cell-depleting therapies in the past 12 months. The increased incidence of prolonged PCR positivity in all patients with hematologic malignancies may be due to reduced antibody titers even in patients who had not received B cell-depleting therapy, possibly because of qualitative defects in B cell function in these patients. Thus, while humoral immunity may not influence viral load early on, they are critical for eventual viral clearance.

Second, we used high-dimensional analysis to identify discrete subgroups of immunologic response to COVID-19 infection. Our analysis identified five groups of patients with distinct T cell differentiation and functional capacity following COVID-19 infection, particularly in the setting of B cell depletion. Notably our results indicate that, while $CD8^+$ T cell function is critical for survival during acute infection, $CD8^+$ T cells alone are not sufficient for efficient viral clearance, as these patients had impaired clearance despite functional and antigen-specific $CD8^+$ T cell immunity. Rather, an immune phenotype associated with efficient viral clearance was defined by an expanded and highly select SARS-CoV-2-specific CD4 T cell clonotype. In the absence of adequate B cell or $CD4^+$ T cell responses, robust $CD8^+$ T cell responses failed to achieve viral clearance. Conversely, in patients with a B cell-depleted phenotype, the presence of a $CD4^+$ T cell response was associated with more efficient viral clearance. This may be due to CD4-dependent coordination of convergent $CD8^+$ T cell responses; $CD4^+$ cells have been shown to enhance memory $CD8^+$ T cell formation (Janssen et al., 2003; Shedlock and Shen, 2003), and in our study, patients in EMD group 1 (which lacked $CD4^+$ T cell responses) also lacked central memory $CD8^+$ differentiation. Alternatively, $CD4^+$ T cells may facilitate residual B cell activity and antibody production (Chen et al., 2010) or enhance the antiviral function of both effector $CD8^+$ T cells and innate immune cells (Karupiah et al., 1996; Topham et al., 1996). This is consistent with data showing that the coordinated presence of both SARS-CoV-2-specific $CD4^+$ and $CD8^+$ T cells correlates with favorable outcomes both during acute infection (Rydyznski Moderbacher et al., 2020) and following recovery (Grifoni et al., 2020). Moreover, severe COVID-19 has been shown to be associated with defective antigen-specific CD4 responses, with decreased clonality and avidity (Bacher et al., 2020).

Limitations of the study

There are several limitations to the present study. Clinical laboratory assays including nasopharyngeal swabs for SARS-CoV-2 RT-PCR, inflammatory markers, and nucleocapsid IgG antibody titers were ordered at the discretion of the treating physician. The timing of research assays including ELISpot, TCR sequencing, and high-dimensional flow cytometry varied according to the timing of first follow-up following clinical improvement and was therefore also somewhat heterogeneous (Figure S1). Finally, the relatively limited number of patients with prolonged infection limited our ability to correlate disease and treatment-associated alterations in immune profiles with prolonged infection.

Nevertheless, our findings underscore the importance of immunologically diverse responses to both viral infection and vaccination. Despite the emergence of SARS-CoV2 variants with decreased sensitivity to antibody-mediated neutralization, mRNA vaccination has remained very effective in protecting patients from both COVID-19 infection and severe disease (Collie et al., 2022; Lopez Bernal et al., 2021). Our data suggest that this is likely attributable to the ability of these vaccines to elicit a robust $CD4^+$ and $CD8^+$ T cell response, which may be of particular importance in protecting against viral infection and disease severity, respectively. Indeed, despite decreased rates of serologic responses to vaccination in patients with hematologic malignancies, studies have demonstrated preserved T cell reactivity to SARS-CoV-2 spike antigens after vaccines (Fendler et al., 2021; Jimenez et al., 2021), and more robust $CD8^+$ T cell responses were observed in patients with rheumatologic conditions receiving anti-CD20 therapies (Gadani et al., 2021; Madelon et al., 2021). The mechanism underlying a stronger cytotoxic T cell response in B cell-depleted patients, whether after COVID-19 infection or SARS-CoV-2 vaccination, is yet to be

(D–F) Depth (D), breadth (E), and convergence (F) of COVID-19 class II-specific TCRs in EMD groups 1, 4, and 2.
(G) Scatterplots of convergence versus breadth of COVID class II-associated TCRs for patients in EMD groups 1, 4, and 2. Gray circles represent TCR repertoires of patients in all other EMD groups.
p values calculated using independent two-sample t test. See also Figure S6.

defined. Furthermore, our data suggest that enhanced $CD8^+$ T cell responses will protect B cell-depleted patients from severe COVID-19 infection but may not efficiently prevent infection or promote rapid clearance in the absence of $CD4^+$ T cell responses. As the novel Omicron variant continues to spread and given early reports indicating conserved Omicron-specific T cell responses (Gao et al., 2022), deeper understanding of $CD4^+$ and $CD8^+$ T cell immunity to viral variants will be key to determining whether currently approved vaccines will continue to be broadly protective against COVID-19 infection and severe disease.

STAR★METHODS

Detailed methods are provided in the online version of this paper and include the following:

- KEY RESOURCES TABLE
- RESOURCE AVAILABILITY
  - Lead contact
  - Materials availability
  - Data and code availability
- EXPERIMENTAL MODEL AND SUBJECT DETAILS
- METHOD DETAILS
  - Immune profiling of patients hospitalized for COVID-19, MSKCC
  - SARS-CoV-2 RNA test
  - Serologic enzyme-linked immunosorbent assay (ELISA)
  - Flow cytometry and statistical analysis
  - High dimensional data analysis of flow cytometry data
  - MHC-I dextramer staining
  - Intracellular cytokine analysis
  - Enzyme-linked immunosorbent (ELISPOT)
  - TCR sequencing
  - Identification of COVID-19 specific TCRs
  - VDJDB set of antigen-specific TCRs
  - Calculating TCR statistics
- QUANTIFICATION AND STATISTICAL ANALYSIS

SUPPLEMENTAL INFORMATION

Supplemental information can be found online at https://doi.org/10.1016/j.ccell.2022.05.013.

ACKNOWLEDGMENTS

A.C.H. was funded by grant CA230157 from the NIH. A.C.H. is supported by the Parker Institute for Cancer Immunotherapy which supports the Cancer Immunology program at the University of Pennsylvania. S.A.V., O.L., Y.E., and B.G. are supported by funding from the Pershing Square Sohn Cancer Research Alliance and the Parker Institute for Cancer Immunotherapy. S.A.V. is supported by the Conrad Hilton Foundation.

AUTHOR CONTRIBUTIONS

A.C.H., B.G., and S.A.V. conceived the project and designed all experiments. M.A.H., E.C., and S.A.V. performed ELISpot and multi-parametric flow-cytometry assays with assistance from P.V. and P.W. for flow cytometry. Y.-H.L. performed class I-specific multimer staining and flow-cytometry-based restimulation assays. S.A.V., J.Y.K., and A.C.H. analyzed flow-cytometry data. O.L., Y.E., A.S., and B.G. analyzed TCR-sequencing data. D.Q., S.R.B., M.D., E.C., and S.A.V. assembled clinical data. N.E.B. performed qPCR experiments for COVID viral load. L.R. performed nucleocapsid IgG testing. S.G. and S.E.H. analyzed COVID-19 patient plasma and provided RBD antibody data. C.B. provided HLA data for dextramer staining. O.L., J.Y.K., D.Q., B.G., A.C.H., and S.A.V. wrote the manuscript. All authors reviewed the manuscript.

DECLARATION OF INTERESTS

S.A.V. is on the advisory board for Immunai and has received consulting fees from ADC Therapeutics. A.C.H. is a consultant for Immunai.

Received: February 18, 2022
Revised: May 6, 2022
Accepted: May 23, 2022
Published: July 11, 2022

REFERENCES

Albiges, L., Foulon, S., Bayle, A., Gachot, B., Pommeret, F., Willekens, C., Stoclin, A., Merad, M., Griscelli, F., Lacroix, L., et al. (2020). Determinants of the outcomes of patients with cancer infected with SARS-CoV-2: results from the Gustave Roussy cohort. Nat Cancer *1*, 965–975. https://doi.org/10.1038/s43018-020-00120-5.

Andreatta, M., and Nielsen, M. (2016). Gapped sequence alignment using artificial neural networks: application to the MHC class I system. Bioinformatics *32*, 511–517. https://doi.org/10.1093/bioinformatics/btv639.

Arcani, R., Colle, J., Cauchois, R., Koubi, M., Jarrot, P.A., Jean, R., Boyer, A., Lachamp, J., Tichadou, A., Couderc, A.L., et al. (2021). Clinical characteristics and outcomes of patients with haematologic malignancies and COVID-19 suggest that prolonged SARS-CoV-2 carriage is an important issue. Ann. Hematol. *100*, 2799–2803. https://doi.org/10.1007/s00277-021-04656-z.

Bacher, P., Rosati, E., Esser, D., Martini, G.R., Saggau, C., Schiminsky, E., Dargvainiene, J., Schröder, I., Wieters, I., Khodamoradi, Y., et al. (2020). Low-avidity CD4(+) T cell responses to SARS-CoV-2 in unexposed individuals and humans with severe COVID-19. Immunity *53*, 1258–1271.e5. https://doi.org/10.1016/j.immuni.2020.11.016.

Bagaev, D.V., Vroomans, R.M.A., Samir, J., Stervbo, U., Rius, C., Dolton, G., Greenshields-Watson, A., Attaf, M., Egorov, E.S., Zvyagin, I.V., et al. (2020). VDJdb in 2019: database extension, new analysis infrastructure and a T-cell receptor motif compendium. Nucleic Acids Res. *48*, D1057–D1062. https://doi.org/10.1093/nar/gkz874.

Bange, E.M., Han, N.A., Wileyto, P., Kim, J.Y., Gouma, S., Robinson, J., Greenplate, A.R., Hwee, M.A., Porterfield, F., Owoyemi, O., et al. (2021). CD8(+) T cells contribute to survival in patients with COVID-19 and hematologic cancer. Nat. Med. *27*, 1280–1289. https://doi.org/10.1038/s41591-021-01386-7.

Carlson, C.S., Emerson, R.O., Sherwood, A.M., Desmarais, C., Chung, M.W., Parsons, J.M., Steen, M.S., LaMadrid-Herrmannsfeldt, M.A., Williamson, D.W., Livingston, R.J., et al. (2013). Using synthetic templates to design an unbiased multiplex PCR assay. Nat. Commun. *4*, 2680. https://doi.org/10.1038/ncomms3680.

Chen, G., Wu, D., Guo, W., Cao, Y., Huang, D., Wang, H., Wang, T., Zhang, X., Chen, H., Yu, H., et al. (2020). Clinical and immunological features of severe and moderate coronavirus disease 2019. J. Clin. Invest. *130*, 2620–2629. https://doi.org/10.1172/JCI137244.

Chen, J., Lau, Y.F., Lamirande, E.W., Paddock, C.D., Bartlett, J.H., Zaki, S.R., and Subbarao, K. (2010). Cellular immune responses to severe acute respiratory syndrome coronavirus (SARS-CoV) infection in senescent BALB/c mice: CD4+ T cells are important in control of SARS-CoV infection. J. Virol. *84*, 1289–1301. https://doi.org/10.1128/JVI.01281-09.

Choi, B., Choudhary, M.C., Regan, J., Sparks, J.A., Padera, R.F., Qiu, X., Solomon, I.H., Kuo, H.H., Boucau, J., Bowman, K., et al. (2020). Persistence and evolution of SARS-CoV-2 in an immunocompromised host. N. Engl. J. Med. *383*, 2291–2293. https://doi.org/10.1056/NEJMc2031364.

Clark, J.J., Dwyer, D., Pinwill, N., Clark, P., Johnson, P., and Hackshaw, A. (2021). The effect of clinical decision making for initiation of systemic anticancer treatments in response to the COVID-19 pandemic in England: a

retrospective analysis. Lancet Oncol. *22*, 66–73. https://doi.org/10.1016/S1470-2045(20)30619-7.

Collie, S., Champion, J., Moultrie, H., Bekker, L.G., and Gray, G. (2022). Effectiveness of BNT162b2 vaccine against omicron variant in South Africa. N. Engl. J. Med. *386*, 494–496. https://doi.org/10.1056/NEJMc2119270.

Dai, M., Liu, D., Liu, M., Zhou, F., Li, G., Chen, Z., Zhang, Z., You, H., Wu, M., Zheng, Q., et al. (2020). Patients with cancer appear more vulnerable to SARS-CoV-2: a multicenter study during the COVID-19 outbreak. Cancer Discov. *10*, 783–791. https://doi.org/10.1158/2159-8290.CD-20-0422.

Dan, J.M., Mateus, J., Kato, Y., Hastie, K.M., Yu, E.D., Faliti, C.E., Grifoni, A., Ramirez, S.I., Haupt, S., Frazier, A., et al. (2021). Immunological memory to SARS-CoV-2 assessed for up to 8 months after infection. Science *371*, eabf4063. https://doi.org/10.1126/science.abf4063.

Emerson, R.O., DeWitt, W.S., Vignali, M., Gravley, J., Hu, J.K., Osborne, E.J., Desmarais, C., Klinger, M., Carlson, C.S., Hansen, J.A., et al. (2017). Immunosequencing identifies signatures of cytomegalovirus exposure history and HLA-mediated effects on the T cell repertoire. Nat. Genet. *49*, 659–665. https://doi.org/10.1038/ng.3822.

Fendler, A., Shepherd, S.T.C., Au, L., Wilkinson, K.A., Wu, M., Byrne, F., Cerrone, M., Schmitt, A.M., Joharatnam-Hogan, N., Shum, B., et al. (2021). Adaptive immunity and neutralizing antibodies against SARS-CoV-2 variants of concern following vaccination in patients with cancer: the CAPTURE study. Nat Cancer *2*, 1305–1320. https://doi.org/10.1038/s43018-021-00274-w.

Gadani, S.P., Reyes-Mantilla, M., Jank, L., Harris, S., Douglas, M., Smith, M.D., Calabresi, P.A., Mowry, E.M., Fitzgerald, K.C., and Bhargava, P. (2021). Discordant humoral and T cell immune responses to SARS-CoV-2 vaccination in people with multiple sclerosis on anti-CD20 therapy. EBioMedicine *73*, 103636. https://doi.org/10.1016/j.ebiom.2021.103636.

Gao, Y., Cai, C., Grifoni, A., Müller, T.R., Niessl, J., Olofsson, A., Humbert, M., Hansson, L., Osterborg, A., Bergman, P., et al. (2022). Ancestral SARS-CoV-2-specific T cells cross-recognize the Omicron variant. Nat. Med. *28*, 472–476. https://doi.org/10.1038/s41591-022-01700-x.

Grifoni, A., Weiskopf, D., Ramirez, S.I., Mateus, J., Dan, J.M., Moderbacher, C.R., Rawlings, S.A., Sutherland, A., Premkumar, L., Jadi, R.S., et al. (2020). Targets of T Cell responses to SARS-CoV-2 coronavirus in humans with COVID-19 disease and unexposed individuals. Cell *181*, 1489–1501.e15. https://doi.org/10.1016/j.cell.2020.05.015.

Hanson, K.E., Caliendo, A.M., Arias, C.A., Englund, J.A., Lee, M.J., Loeb, M., Patel, R., El Alayli, A., Kalot, M.A., Falck-Ytter, Y., et al. (2020). Infectious diseases society of America guidelines on the diagnosis of COVID-19. Clin. Infect. Dis. ciaa760. https://doi.org/10.1093/cid/ciaa760.

Hoffmann, M., Arora, P., Groß, R., Seidel, A., Hörnich, B.F., Hahn, A.S., Krüger, N., Graichen, L., Hofmann-Winkler, H., Kempf, A., et al. (2021). SARS-CoV-2 variants B.1.351 and P.1 escape from neutralizing antibodies. Cell *184*, 2384–2393.e12. https://doi.org/10.1016/j.cell.2021.03.036.

Janssen, E.M., Lemmens, E.E., Wolfe, T., Christen, U., von Herrath, M.G., and Schoenberger, S.P. (2003). CD4+ T cells are required for secondary expansion and memory in CD8+ T lymphocytes. Nature *421*, 852–856. https://doi.org/10.1038/nature01441.

Jiménez, M., Roldán, E., Fernández-Naval, C., Villacampa, G., Martinez-Gallo, M., Medina-Gil, D., Peralta-Garzón, S., Pujadas, G., Hernández, C., Pagès, C., Gironella, M., Fox, L., Orti, G., Barba, P., Pumarola, T., Cabirta, A., Catalá, E., Valentín, M., Marín-Niebla, A., Orfao, A., González, M., Campins, M., Ruiz-Camps, I., Valcárcel, D., Bosch, F., Hernández, M., Crespo, M., Esperalba, J., and Abrisqueta, P. (2022). Cellular and humoral immunogenicity of the mRNA-1273 SARS-CoV-2 vaccine in patients with hematologic malignancies. Blood Adv. *6*, 774–784. https://doi.org/10.1182/bloodadvances.2021006101.

Kared, H., Redd, A.D., Bloch, E.M., Bonny, T.S., Sumatoh, H., Kairi, F., Carbajo, D., Abel, B., Newell, E.W., Bettinotti, M.P., et al. (2021). SARS-CoV-2-specific CD8+ T cell responses in convalescent COVID-19 individuals. J. Clin. Invest. *131*, 145476. https://doi.org/10.1172/JCI145476.

Karupiah, G., Buller, R.M., Van Rooijen, N., Duarte, C.J., and Chen, J. (1996). Different roles for CD4+ and CD8+ T lymphocytes and macrophage subsets in the control of a generalized virus infection. J. Virol. *70*, 8301–8309. https://doi.org/10.1128/JVI.70.12.8301-8309.1996.

Kedzierska, K., Venturi, V., Valkenburg, S.A., Davenport, M.P., Turner, S.J., and Doherty, P.C. (2008). Homogenization of TCR repertoires within secondary CD62L^{high} and CD62L^{low} virus-specific CD8^{+} T cell populations. J. Immunol. *180*, 7938–7947. https://doi.org/10.4049/jimmunol.180.12.7938.

Klinger, M., Kong, K., Moorhead, M., Weng, L., Zheng, J., and Faham, M. (2013). Combining next-generation sequencing and immune assays: a novel method for identification of antigen-specific T cells. PLoS One *8*, e74231. https://doi.org/10.1371/journal.pone.0074231.

Klinger, M., Pepin, F., Wilkins, J., Asbury, T., Wittkop, T., Zheng, J., Moorhead, M., and Faham, M. (2015). Multiplex identification of antigen-specific T cell receptors using a combination of immune assays and immune receptor sequencing. PLoS One *10*, e0141561. https://doi.org/10.1371/journal.pone.0141561.

Laing, A.G., Lorenc, A., Del Molino Del Barrio, I., Das, A., Fish, M., Monin, L., Muñoz-Ruiz, M., McKenzie, D.R., Hayday, T.S., Francos-Quijorna, I., et al. (2020). A dynamic COVID-19 immune signature includes associations with poor prognosis. Nat. Med. *26*, 1623–1635. https://doi.org/10.1038/s41591-020-1038-6.

Lee, C.Y., Shah, M.K., Hoyos, D., Solovyov, A., Douglas, M., Taur, Y., Maslak, P., Babady, N.E., Greenbaum, B., Kamboj, M., and Vardhana, S.A. (2022). Prolonged SARS-CoV-2 infection in patients with lymphoid malignancies. Cancer Discov. *12*, 62–73. https://doi.org/10.1158/2159-8290.CD-21-1033.

Lopez Bernal, J., Andrews, N., Gower, C., Gallagher, E., Simmons, R., Thelwall, S., Stowe, J., Tessier, E., Groves, N., Dabrera, G., et al. (2021). Effectiveness of covid-19 vaccines against the B.1.617.2 (Delta) variant. N. Engl. J. Med. *385*, 585–594. https://doi.org/10.1056/NEJMoa2108891.

Madelon, N., Lauper, K., Breville, G., Sabater Royo, I., Goldstein, R., Andrey, D.O., Grifoni, A., Sette, A., Kaiser, L., Siegrist, C.A., et al. (2021). Robust T cell responses in anti-CD20 treated patients following COVID-19 vaccination: a prospective cohort study. Clin. Infect. Dis. ciab954. https://doi.org/10.1093/cid/ciab954.

Malek, T.R. (2008). The biology of interleukin-2. Annu. Rev. Immunol. *26*, 453–479. https://doi.org/10.1146/annurev.immunol.26.021607.090357.

Mathew, D., Giles, J.R., Baxter, A.E., Oldridge, D.A., Greenplate, A.R., Wu, J.E., Alanio, C., Kuri-Cervantes, L., Pampena, M.B., D'Andrea, K., et al. (2020). Deep immune profiling of COVID-19 patients reveals distinct immunotypes with therapeutic implications. Science *369*. https://doi.org/10.1126/science.abc8511.

Minervina, A.A., Komech, E.A., Titov, A., Bensouda Koraichi, M., Rosati, E., Mamedov, I.Z., Franke, A., Efimov, G.A., Chudakov, D.M., Mora, T., et al. (2021). Longitudinal high-throughput TCR repertoire profiling reveals the dynamics of T-cell memory formation after mild COVID-19 infection. Elife *10*, e63502. https://doi.org/10.7554/eLife.63502.

Mudd, P.A., Minervina, A.A., Pogorelyy, M.V., Turner, J.S., Kim, W., Kalaidina, E., Petersen, J., Schmitz, A.J., Lei, T., Haile, A., et al. (2022). SARS-CoV-2 mRNA vaccination elicits a robust and persistent T follicular helper cell response in humans. Cell *185*, 603–613.e15. https://doi.org/10.1016/j.cell.2021.12.026.

Nolan, S., Vignali, M., Klinger, M., Dines, J.N., Kaplan, I.M., Svejnoha, E., Craft, T., Boland, K., Pesesky, M., Gittelman, R.M., et al. (2020). A large-scale database of T-cell receptor beta (TCRβ) sequences and binding associations from natural and synthetic exposure to SARS-CoV-2. Res. Sq. https://doi.org/10.21203/rs.3.rs-51964/v1.

Peng, Y., Mentzer, A.J., Liu, G., Yao, X., Yin, Z., Dong, D., Dejnirattisai, W., Rostron, T., Supasa, P., Liu, C., et al. (2020). Broad and strong memory CD4(+) and CD8(+) T cells induced by SARS-CoV-2 in UK convalescent individuals following COVID-19. Nat. Immunol. *21*, 1336–1345. https://doi.org/10.1038/s41590-020-0782-6.

Pfizenmaier, K., Scheurich, P., Däubener, W., Krönke, M., Röllinghoff, M., and Wagner, H. (1984). Quantitative representation of all T cells committed to develop into cytotoxic effector cells and/or interleukin 2 activity-producing helper cells within murine T lymphocyte subsets. Eur. J. Immunol. *14*, 33–39. https://doi.org/10.1002/eji.1830140107.

Planas, D., Veyer, D., Baidaliuk, A., Staropoli, I., Guivel-Benhassine, F., Rajah, M.M., Planchais, C., Porrot, F., Robillard, N., Puech, J., et al. (2021). Reduced

sensitivity of SARS-CoV-2 variant Delta to antibody neutralization. Nature *596*, 276–280. https://doi.org/10.1038/s41586-021-03777-9.

Ranganathan, P., Sengar, M., Chinnaswamy, G., Agrawal, G., Arumugham, R., Bhatt, R., Bilimagga, R., Chakrabarti, J., Chandrasekharan, A., Chaturvedi, H.K., et al. (2021). Impact of COVID-19 on cancer care in India: a cohort study. Lancet Oncol. *22*, 970–976. https://doi.org/10.1016/S1470-2045(21)00240-0.

Rodda, L.B., Netland, J., Shehata, L., Pruner, K.B., Morawski, P.A., Thouvenel, C.D., Takehara, K.K., Eggenberger, J., Hemann, E.A., Waterman, H.R., et al. (2021). Functional SARS-CoV-2-specific immune memory Persists after mild COVID-19. Cell *184*, 169–183.e17. https://doi.org/10.1016/j.cell.2020.11.029.

Rydyznski Moderbacher, C., Ramirez, S.I., Dan, J.M., Grifoni, A., Hastie, K.M., Weiskopf, D., Belanger, S., Abbott, R.K., Kim, C., Choi, J., et al. (2020). Antigen-specific adaptive immunity to SARS-CoV-2 in acute COVID-19 and associations with age and disease severity. Cell *183*, 996–1012.e19. https://doi.org/10.1016/j.cell.2020.09.038.

Satish, T., Raghunathan, R., Prigoff, J.G., Wright, J.D., Hillyer, G.A., Trivedi, M.S., Kalinsky, K., Crew, K.D., Hershman, D.L., and Accordino, M.K. (2021). Care Delivery impact of the COVID-19 pandemic on breast cancer care. JCO Oncol. Pract. *17*, e1215–e1224. https://doi.org/10.1200/OP.20.01062.

Sekine, T., Perez-Potti, A., Rivera-Ballesteros, O., Strålin, K., Gorin, J.B., Olsson, A., Llewellyn-Lacey, S., Kamal, H., Bogdanovic, G., Muschiol, S., et al. (2020). Robust T cell immunity in convalescent individuals with asymptomatic or mild COVID-19. Cell *183*, 158–168.e14. https://doi.org/10.1016/j.cell.2020.08.017.

Shedlock, D.J., and Shen, H. (2003). Requirement for CD4 T cell help in generating functional CD8 T cell memory. Science *300*, 337–339. https://doi.org/10.1126/science.1082305.

Snyder, T.M., Gittelman, R.M., Klinger, M., May, D.H., Osborne, E.J., Taniguchi, R., Zahid, H.J., Kaplan, I.M., Dines, J.N., Noakes, M.N., et al. (2020). Magnitude and dynamics of the T-cell response to SARS-CoV-2 infection at both individual and population levels. Preprint at medRxiv. https://doi.org/10.1101/2020.07.31.20165647.

Tham, E.L., and Mescher, M.F. (2002). The poststimulation program of CD4 versus CD8 T cells (death versus activation-induced nonresponsiveness). J. Immunol. *169*, 1822–1828. https://doi.org/10.4049/jimmunol.169.4.1822.

Topham, D.J., Tripp, R.A., Sarawar, S.R., Sangster, M.Y., and Doherty, P.C. (1996). Immune CD4+ T cells promote the clearance of influenza virus from major histocompatibility complex class II -/- respiratory epithelium. J. Virol. *70*, 1288–1291. https://doi.org/10.1128/JVI.70.2.1288-1291.1996.

Wang, P., Nair, M.S., Liu, L., Iketani, S., Luo, Y., Guo, Y., Wang, M., Yu, J., Zhang, B., Kwong, P.D., et al. (2021). Antibody resistance of SARS-CoV-2 variants B.1.351 and B.1.1.7. Nature *593*, 130–135. https://doi.org/10.1038/s41586-021-03398-2.

Zeng, F., Wu, M., Wang, J., Li, J., Hu, G., and Wang, L. (2021). Over 1-year duration and age difference of SARS-CoV-2 antibodies in convalescent COVID-19 patients. J. Med. Virol. *93*, 6506–6511. https://doi.org/10.1002/jmv.27152.

STAR★METHODS

KEY RESOURCES TABLE

REAGENT or RESOURCE	SOURCE	IDENTIFIER
Antibodies		
CR3022 (IgG monoclonal antibody to SARS-CoV-2 spike protein)	Hensley Lab	N/A
UltraComp eBeads	ThermoFisher	01-2222-42
CD45RA-BUV395	BD Biosciences	740,298
PD-1-BV421	BioLegend	329,920
IgD-BV480	BD Biosciences	566,138
CXCR5-BB515	BD Biosciences	564,624
CD8-BUV496	BD Biosciences	612,943
CD19-BUV563	BD Biosciences	612,916
CD3-BV570	BioLegend	300,436
CD16-BUV615	BD Biosciences	751,572
CD138-BV605	BioLegend	356,520
Eomes-PE-eFluor610	Invitrogen	61-4877-42
TCF-1-Alexa647	Cell Signaling	6709S
CD38-BUV661	BD Biosciences	612,969
CD95-BV650	BioLegend	305,642
CCR7-BB700	BD Biosciences	566,437
CD21-BV711	BD Biosciences	563,163
Ki-67-Alexa700	BD Biosciences	561,277
CD27-BUV737	BD Biosciences	612,829
CD4-BV750	BD Biosciences	566,355
CX3CR1-biotin	BioLegend	341,617
Streptavidin-BB790	BD Biosciences	Custom
CD39-APC/Fire750	BioLegend	328,230
T-bet-PE/Cy7	BioLegend	644,824
HLA-DR-BV786	BD Biosciences	564,041
CD20-BUV805	BD Biosciences	612,905
TOX-PE	Miltenyi	130-120-716
ICOS-PE-Cy5	Thermo Fisher	15-9949-82
IFN-g-FITC	BioLegend	502,506
TNF-a-PE	BioLegend	502,909
IL-2-BV421	BioLegend	503,826
Biological samples		
Patient PBMCs	MSKCC	IRB
Chemicals, peptides, and recombinant proteins		
Peptivator EBV consensus peptides	Miltenyi	130-099-764
Peptivator SARS-CoV-2 Select	Miltenyi	130-127-309
GhostDye 510 (Viability dye)	Tonbo Biosciences	13–0780
Human TruStain FcX	BioLegend	422,302
Dasatinib	Selleck Chemicals	S1021
MHC Dextramer SARS-CoV-2 Spike Panel-S PE	Immudex	RX06-PE-150
FoxP3 Intracellular Staining Kit	eBioscience	00-5523-00

(*Continued on next page*)

Continued

REAGENT or RESOURCE	SOURCE	IDENTIFIER
Critical commercial assays		
TaqPath™ COVID-19 Combo Kit	Thermo Fisher	A47814
cobas® SARS-CoV-2 test	Roche Diagnostics	23-312-207
Xpert Xpress SARS-CoV-2 test	Cepheid	https://www.cepheid.com/coronavirus
SpectraMax 190 microplate reader	Molecular Devices	https://www.moleculardevices.com/products/microplate-readers/absorbance-readers
Architect i2000 analyzer	Abbott	https://www.corelaboratory.abbott/us/en/offerings/brands/architect/architect-i2000SR
FACSSymphony A5 Cell Analyzer	BD Biosciences	https://www.bdbiosciences.com/en-us/products/instruments/flow-cytometers/research-cell-analyzers/bd-facsymphony-a5
S6 Analyzer	Immunospot	https://immunospot.com/products/analyzers
immunoSEQ Assay	Adaptive Biotechnologies	Carlson et al. (2013); Emerson et al. (2017)
Cytek Aurora Spectral Cytometer	Cytek	https://cytekbio.com/pages/aurora
MIRA Assay	Illumina	Klinger et al. (2013); Klinger et al. (2015)
Human IFN-γ/IL-2 Double-Color ELISPOT plates	Immunospot	https://immunospot.com/human-ifn-gamma-il-2-double-color-elispot.html
Deposited data		
De-identified patient data	This paper	https://doi.org/10.17632/869vkpzc3f.1
immunoSEQ® T-MAP™ COVID database	Adaptive Biotechnologies	https://www.immunoseq.com/tmap-covid/
VDJDB Database (downloaded on July 27, 2021)	https://vdjdb.cdr3.net/	Bagaev et al. (2020)
TCR statistics including COVID-19-specific TCR breadth, depth, clonality, convergence	This paper	N/A
Software and algorithms		
Prism version 9	GraphPad Software	https://www.graphpad.com/
Excel	Microsoft Office Suite	https://www.microsoft.com/en-us/microsoft-365/excel
R statistical software	RStudio	https://www.rstudio.com/
R package 'rpart'	CRAN	https://cran.r-project.org/package=rpart
Omiq	Omiq	https://omiq.ai
R package 'emdist'	CRAN	https://cran.r-project.org/package=emdist
FlowJo 10.0 software	BD Biosciences	https://www.flowjo.com/

RESOURCE AVAILABILITY

Lead contact

- Further information and requests for resources and reagents should be directed to and will be fulfilled by the lead contact, Santosha Vardhana (vardhans@mskcc.org).

Materials availability

- This study did not generate new unique reagents.

Data and code availability

- DOIs are listed in the key resources table.
- De-identified patient data can be found in Table S1 and is publicly available as of the date of publication.
- Additional Supplemental Items are available from Mendeley Data at https://doi.org/10.17632/869vkpzc3f.1
- Any additional information required to reanalyze the data reported in this paper is available from the lead contact upon request.

EXPERIMENTAL MODEL AND SUBJECT DETAILS

Adult patients (≥18 years) with cancer who were seen at Memorial Sloan Kettering Cancer Center, with a prior SARS-CoV-2 positive PCR test, either directly assessed at Memorial Sloan Cancer Center or officially reported in the electronic medical record, met criteria for convalescence as defined by clinical improvement from peak symptoms, and consented to MSKCC IRB #06-107 ("Storage and

Research Use of Human Biospecimens") between March 1, 2020 and January 20, 2021 were eligible for inclusion. Details on age, sex and other clinical characteristics are available in paragraphs 1-3 of the Results section and in Table 1 of the manuscript.

METHOD DETAILS

Immune profiling of patients hospitalized for COVID-19, MSKCC

Patients with a prior SARS-CoV-2 positive PCR test, either directly assessed at Memorial Sloan Cancer Center or officially reported in the electronic medical record, met criteria for convalescence as defined by clinical improvement from peak symptoms, and consented to MSKCC IRB #06-107 ("Storage and Research Use of Human Biospecimens") between March 1, 2020 and January 20, 2021 were eligible for inclusion. Identification of case-patients and their medical background and clinical course during COVID-19 illness were abstracted from electronic medical records.

SARS-CoV-2 RNA test

SARS-CoV-2 RNA was detected in nasopharyngeal swabs (NPS) or saliva samples using a laboratory-developed test as previously described. (4,38) Testing was also performed using several commercial assays including the TaqPath COVID-19 Combo Kit (Thermo Fisher Scientific, Waltham, MA) targeting the N, S and ORF genes, the cobas SARS-CoV-2 test (Roche Molecular Diagnostics, Indianapolis, IN) targeting the ORF1 a/b and E gene and the Xpert Xpress SARS-CoV-2 test (Cepheid, Sunnyvale, California) targeting the N and E genes. Samples were reported as positive per manufacturers' instructions. The cycle threshold (Ct) value, a semi-quantitative estimate of the viral SARS-CoV-2 RNA load, was retrieved for all gene targets from each instrument record.

Serologic enzyme-linked immunosorbent assay (ELISA)

Spike protein receptor binding domain

ELISAs were completed using plates coated with the receptor binding domain (RBD) of the SARS-CoV-2 spike protein as previously described[47]. Briefly, Prior to testing, plasma and serum samples were heat-inactivated at 56 °C for 1 hour. Plates were read at an optical density (OD) of 450 nm using the SpectraMax 190 microplate reader (Molecular Devices). Background OD values from the plates coated with PBS were subtracted from the OD values from plates coated with recombinant protein. Each plate included serial dilutions of the IgG monoclonal antibody CR3022, which is reactive to the SARS-CoV-2 spike protein, as a positive control to adjust for inter assay variability. Plasma and serum antibody concentrations were reported as arbitrary units relative to the CR3022 monoclonal antibody. A cutoff of 0.48 arbitrary units was established from a 2019 cohort of pre-pandemic individuals and used for defining seropositivity.

Nucleocapsid

IgG antibodies to SARS-CoV-2 in serum were determined on the Architect i2000 analyzer using a two-step automated chemiluminescent microparticle immunoassay (CMIA) technology. The presence or absence of IgG antibodies to SARS-CoV-2 in the sample was determined by comparing the chemiluminescent relative light units (RLU) in the reaction to the calibrator RLU.

Flow cytometry and statistical analysis

Samples were acquired on a 5 laser BD FACS Symphony A5. UltraComp eBeads (ThermoFisher, Cat#01-2222-42) were used for compensation. Up to 2 × 10^6 live PBMC were acquired per each sample. Due to the heterogeneity of clinical and flow cytometric data, non-parametric tests of association were preferentially used throughout the study. Tests of association between mixed continuous variables versus non-ordered categorical variables (n = 2) were performed by Mann-Whitney test. Tests of association between binary variables versus non-ordered categorical variables (n = 2) were performed using Pearson Chi Square test. All tests were performed using a nominal significance threshold of $P < 0.05$ with Prism version 9 (GraphPad Software) and Excel (Microsoft Office Suite). Classification and Regression Tree analysis (CART) was performed using R package 'rpart'.

High dimensional data analysis of flow cytometry data

UMAP and FlowSOM analyses were conducted using the online platform Omiq (https://omiq.ai) Lymphocytes, CD8 T-cells, and CD4 T-cells were analyzed separately. UMAP analysis was performed using downsampling of at most 10,000 cells from each FCS file in lymphocytes, CD8 T-cells, and CD4 T-cells. UMAP analysis for lymphocytes was performed with a nearest neighbors of 50, minimum distance of 0.01, number of components of 2 and a Euclidean metric. UMAP analyses for CD8 T-cells and CD4 T-cells were performed with a nearest neighbors of 50, minimum distance of 0.25, number of components of 2 and a Euclidean metric. These UMAPs were the basis for the downstream FlowSOM clustering algorithm on Omiq. A new self-organizing map (SOM) was generated for lymphocytes, CD8 T-cells, and CD4 T-cells using hierarchical consensus clustering. For each SOM, 225 clusters and ten metaclusters were identified. For lymphocytes, the following markers were used in the UMAP and FlowSOM analyses: CD45RA, PD-1, IgD, CXCR5, CD8, CD19, CD3, CD16, CD138, Eomes, TCF-1, CD38, CD95, CCR7, CD21, Ki-67, CD27, CD4, CX3CR1, CD39, T-bet, HLA-DR, CD20, TOX, and ICOS. For CD8 T-cells and CD4 T-cells, the following markers were used: CD45RA, PD-1, CXCR5, Eomes, TCF-1, CD38, CCR7, Ki-67, CD27, CX3CR1, CD39, Tbet, HLA-DR, TOX, ICOS, and CD95. Heat maps were created using the Omiq figure function.

To group individuals based on lymphocyte landscape, pairwise EMD values were calculated on the lymphocyte UMAP axes using the emdist package in R. Resulting scores were hierarchically clustered using the hclust function in the stats package in R. EMD and

UMAP projects was created for 66 subjects. However, 63 had clinical annotations available, and were selected for downstream analyses.

MHC-I dextramer staining

PBMCs were thawed and stained with a viability dye (GhostDye 510) and Fc Block. They were then washed and pre-incubated with dasatinib, 100 nM for 10 minutes at 37C prior to staining with pooled SARS-CoV-2 class I-specific dextramers (Immudex) or control dextramers for 20 minutes, and were subsequently stained with surface markers for immunophenotyping, including CD45RA, CD8, CD19, CD3, CD16, CD38, CCR7, CD27, CD4, and HLA-DR. Samples were acquired using a Cytek Aurora Spectral Cytometer and analyzed using FlowJo 10.0 software.

Intracellular cytokine analysis

PBMCs were thawed and incubated at 37C in T-cell media (RPMI + 10% fetal bovine serum, penicillin/streptomycin, L-glutamine, beta-mercaptoethanol) and with or without peptide (Miltenyi Peptivator EBV consensus or SARS-CoV-2 Select) at a final concentration of 0.3 micromolar. Two hours later, brefeldin A was added to cultures and cells were incubated an additional three hours. Cells were harvested and stained with viability dye and Fc Block as above, followed by surface markers including CD45RA, CD8, CD19, CD3, CD16, CD38, CCR7, CD27, CD4, and HLA-DR. Cells were fixed, permeabilized, and intracellularly stained for IFN-g, TNF-a and IL-2 using a FoxP3 intracellular staining kit (eBioscience). Samples were acquired using a Cytek Aurora Spectral Cytometer and analyzed using FlowJo 10.0 software.

Enzyme-linked immunosorbent (ELISPOT)

ELISPOT assays: 100,000 PBMCs per well were plated on Human IFN-γ/IL-2 Double-Color ELISPOT plates (Immunospot) in the presence of anti-human CD28 (0.2 ug/mL) and with or without peptide (Miltenyi Peptivator EBV consensus or SARS-CoV-2 Select) at a final concentration of 0.3 micromolar. The EBV consensus pool (130-099-764) contains 43 MHC class I and class II peptides derived from 13 EBV proteins while the SARS-CoV-2 select peptide pool (130-127-309) contains 88 lyophilized MHC class I and class I restricted peptides derived from the whole proteome of SARS-CoV-2. Plates were incubated in a 37C humidified incubator for 18 hours, after which plates were stained as per manufacturer's instructions and quantified using an automated ImmunoSpot S6 Analyzer. Results are expressed in Spot Forming Units (SFU) per 10^6 PBMCs.

TCR sequencing

Immunosequencing of the CDR3 regions of human TCRβ chains was performed on genomic DNA from PBMC samples using the immunoSEQ Assay (Adaptive Biotechnologies) as previously described (Carlson et al., 2013; Emerson et al., 2017). In brief, genomic DNA was extracted from PBMC samples, amplified in a bias-controlled multiplex PCR, followed by high-throughput sequencing, identification and quantification of absolute abundances of unique TCRβ CDR3 regions.

Identification of COVID-19 specific TCRs

Attribution of SARS-CoV-2 antigen specificities was assigned to TCR sequences according to the immunoSEQ T-MAP COVID database by Adaptive Biotechnologies (Nolan et al., 2020) which includes over 135,000 TCR sequences identified as reactive to SARS-CoV-2 class I or class II epitopes using the MIRA assay (Klinger et al., 2013, 2015). Briefly, to identify antigen-specific TCRs, T-cells from over 1,400 subjects exposed to or infected with the SARS-CoV-2 virus were incubated in a combinatorial fashion with SARS-CoV-2 peptide pools, and the antigen-specific subset of TCRs in each experiment was identified by CD137 upregulation and reported in the immunoSEQ T-MAP COVID database. Clones in the TCR sequenced samples of patients in this cohort were assigned to COVID-19 class I-specific or class II-specific subsets if the CDR3 regions of their TCR sequences matched CDR3 regions of TCR sequences included in the class I or class II subsets of the immunoSEQ T-MAP COVID database, respectively.

VDJDB set of antigen-specific TCRs

VDJDB is a curated publicly available database of TCR sequences with experimentally identified antigen specificities (Bagaev et al., 2020). The largest sets of TCRs in this dataset are associated with CMV, Influenza A, and EBV. We used TCRs with known specificities from VDJDB (downloaded on July 27, 2021), excluding those reported in VDJDB as SARS-CoV-2 specific, to compare TCR statistics of SARS-CoV-2 associated TCRs and those associated with other known antigens.

Calculating TCR statistics

Breadth, depth, clonality, and convergence of COVID-19 class I and class II-specific TCRs, as well as clonality and convergence of the TCR repertoires overall, were calculated for each TCR sequenced sample.

Clonal breadth characterizes how many unique TCR clones in a TCR repertoire belong to a TCR sequence subset of interest, namely COVID-19 class I or class II-specific TCRs, and is calculated following the approach described in (Snyder et al., 2020): $Breadth = \frac{1}{N}\sum_{i \in S} 1$, where N is the number of unique TCR clones (identified by a unique CDR3 sequence among productive TCR reads) in a repertoire D, and S is the TCR subset of interest (COVID-19 class I or class II specific TCRs).

Clonal depth characterizes what fraction of all productive TCR reads in a TCR repertoire is occupied by TCRs belonging to a TCR subset of interest: $Depth = \sum_{i \in S} p_i$, where $p_i = \frac{n_i}{\sum_{j \in D} n_j}$ is the productive frequency of clone i; n_i is the count of reads belonging to clone i; jεD are all clones in TCR repertoire D, and i$\in$ S are all clones in TCR repertoire D that belong to subset S of interest.

TCR clonality is a measure of TCR repertoire diversity and is calculated as 1 - normalized Shannon entropy: $Clonality = 1 - H$ and $H = \frac{-\sum_{i \in D} p_i \log_2(p_i)}{\log_2(M)}$, where H is normalized Shannon entropy, p_i is the productive frequency of clone i in TCR repertoire D as defined above, and M is the total number of reads of detected TCR clones (total number of productive TCR reads). TCR clonality was calculated for the TCR repertoire overall as well as clones belonging to a TCR subset S of interest: $Clonality_S = 1 - H_S$ and $H_S = \frac{-\sum_{i \in S} p_i \log_2(p_i)}{\log_2(M_S)}$, where H_S is the normalized Shannon entropy for TCR subset S and M_S is the total number of reads for TCR clones in subset S.

TCR convergence is a proposed measure of selection which measures how many different TCR recombination events result in a functionally similar T-cell clone, as defined by the same CDR3 sequence, calculated as $Convergence = 1 - \frac{N}{K}$, where N is the number of unique TCR clones as defined by unique amino acid CDR3 sequences and K is the number of unique TCR clones as defined by unique nucleotide CDR3 sequences. As with clonality, TCR convergence was calculated for the repertoire overall as well as for TCR subsets of interest, namely SARS-CoV-2 class-I and class-II specific TCRs: $Convergence_S = 1 - \frac{N_S}{K_S}$, where S is a TCR subset of interest, and N_S and K_S are the number of unique amino acid CDR3 sequences and unique nucleotide CDR3 sequences, respectively, of TCRs in a repertoire that belong to the subset S.

QUANTIFICATION AND STATISTICAL ANALYSIS

Quantification and statistical analyses were performed using GraphPad Prism v9.3.1. Statistical tests were performed as indicated in Figure legends.